



Gramos Muja, BSc

**Investigation of hardening-induced macrocracking by
implementation of a discrete failure plane in thermo-mechanical
3D Finite Element models**

MASTER'S THESIS

to achieve the university degree of

Diplom-Ingenieur

Master's degree programme: Civil Engineering and Structural Engineering

submitted to

Graz University of Technology

Supervisor

Ass.Prof. Dipl.-Wirtsch.-Ing. Dr.techn. Dirk Schlicke

Institute of Structural Concrete

Faculty of Civil Engineering Sciences

Graz, August 2017

AFFIDAVIT

I declare that I have authored this thesis independently, that I have not used other than the declared sources/resources, and that I have explicitly indicated all material which has been quoted either literally or by content from the sources used. The text document uploaded to TUGRAZonline is identical to the present master's thesis.

29.08.2017

Date

Gramos Muja

Signature

Die Erstellung dieser Masterarbeit wurde von der Bundesanstalt für Wasserbau (BAW) unterstützt.

The preparation of this master thesis was supported by the Federal Waterways Engineering and Research Institute (BAW).

Acknowledgment

I would like to thank my thesis supervisor Ass.Prof. Dr. techn. Dirk Schlicke for the engagement, comments and relentless support. The door to Prof. Schlicke's office was always for me whenever I had a question or needed his experience. I also would like to thank all the members of the Institute for Structural Concrete and especially Dr. techn. Katrin Turner, Dipl.-Ing. Peter Joachim Heinrich for the insightful discussions.

I would like to express my gratitude to my friends from the Hydraulic Engineering Drawing Studio for the good times and unforgettable moments that we shared. I will always remember the joy that I felt here.

The biggest thank you goes however to my family. I want to express my gratitude towards my mother Lumturije and my father Enver for their love, patience, care and for always putting the needs of their children over their own.

Finally I want to thank my brother Gjin without whom this all wouldn't have been possible. Thank you for the continuous encouragement throughout the years. Thank you for your help through university and most of all thank you for being the best brother that anyone can have.

Gramos Muja

Abstract

As a result of concrete hardening, restraint stresses can occur, which can lead to cracking. The reason for this crack formation is the deformation behavior of the concrete during hydration, environmental influences and the degree of restraint. The assessment of the risk of cracking is generally based on thermomechanical 3D calculation models without consideration of crack formation.

The first part of this thesis deals with the implementation of a discrete plane of failure in such thermomechanical 3D calculation models in order to enable the investigation of cracking on the basis of realistic stress states in the decisive cross section of the member. A special emphasis was placed on the consideration of softening behavior in the cracking process of the concrete in order to be able to depict the reduction of the restraint stresses by the initial crack opening.

The final model allows systematic investigations of the reduction of eigenstresses due to local failure in the cross section as well as the formation of macrocracks as a result of critical restraint forces. To illustrate this possibility, the second part of this work contains a case study on two typical structural members. On the one hand, a very massive block without significant external restraint was simulated, in which surface cracks can be formed only as a result of the eigenstresses. On the other hand, a thick wall on a foundation was simulated, in which larger separating cracks occur with increasing length due to the external restraint.

Kurzfassung

Infolge der Betonehärtung können Zwangbeanspruchungen auftreten, die in weiterer Folge zur Rissbildung führen können. Ursächlich für diese Rissbildung sind das Verformungsverhalten des Betons während der Hydratation, äußere Einflüsse gemäß der Umweltbedingungen und der Behinderungsgrad des Bauteils. Die Beurteilung der Rissgefahr erfolgt im Allgemeinen auf Grundlage von thermomechanischen 3D-Berechnungsmodellen ohne Berücksichtigung der Rissbildung.

Der erste Teil der vorliegenden Arbeit beschäftigt sich mit der Implementierung einer diskreten Rissebene in solche thermomechanischen 3D-Berechnungsmodelle, um die Rissbildung auf Basis von realistischen Spannungszuständen im Bauteilquerschnitt untersuchen zu können. Hierbei wurde besonderer Wert auf die Berücksichtigung des Softening-Verhaltens im Rissbildungsprozess des Betons gelegt, um den Abbau der Zwangbeanspruchung durch die beginnende Rissöffnung abbilden zu können.

Das endgültige Modell ermöglicht systematische Untersuchungen sowohl der Reduktion von Eigenspannungen durch lokales Versagen im Querschnitt als auch Makrorissbildung als Folge kritischer Risschnittgrößen. Zur Veranschaulichung dieser Möglichkeit wurde im zweiten Teil dieser Arbeit eine Fallstudie an zwei typischen Bauteilsituationen durchgeführt. Zum einen wurde ein sehr massiges Bauteil ohne nennenswerte äußere Behinderung abgebildet, in dem sich allein infolge der Eigenspannungen ausgeprägte Schalenrisse bilden können. Zum anderen wurde eine dicke Wand auf Fundament betrachtet, bei der aufgrund der äußeren Behinderung mit zunehmender Länge eine größere Trennrissbildung zu erwarten ist.

Contents

1	Introduction	1
1.1	State of the Art	1
1.1.1	General member behavior in the uncracked state	1
1.1.2	Analytical prediction of crack formation on basis of stress distribution	3
1.2	Motivation and objectives	5
1.3	General approach	6
2	Relevant material behavior and its computational consideration	8
2.1	Thermo-mechanical behavior of hardening concrete	8
2.1.1	Preliminary remarks	8
2.1.2	Maturity, heat release and evolution of thermal properties	8
2.1.3	Evolution of mechanical properties	9
2.1.4	Coupling and material model for computational purposes	9
2.2	Behaviour under tension	9
2.2.1	Stress-strain relation in the uncracked state	10
2.2.2	Crack opening and fracture energy	10
3	Discrete crack modeling	12
3.1	General remarks	12
3.2	Applied approaches	13
3.2.1	"Element cut-off" without softening	13
3.2.2	Softening fracture	14
4	Case study	16
4.1	General remarks	16
4.2	Large concrete foundation	17
4.2.1	Specifications of the example	17
4.2.2	Calculation model	18
4.2.3	Hardening-induced temperature and stress history	19
4.2.4	Influence of soil stiffness	22
4.2.5	Discrete crack analysis with "element cut-off" approach	24
4.2.6	Discrete crack analysis with softening approach	25
4.3	Wall on foundation	26
4.3.1	Specification of the example	26
4.3.2	Calculation modell	27
4.3.3	Hardening induced temperature and stress history	29
4.3.4	Discrete Crack analysis with softening approach	33

5	Discussion	37
5.1	Crack formation in very thick members with negligible external restraint . .	37
5.2	Crack formation in walls on foundations	39
5.2.1	General remarks	39
5.2.2	Influence of L/H	40
5.2.3	Influence of foundation stiffness	41
6	Conclusion	44

1 Introduction

Concrete is one of the most applied building materials due to its appropriate mechanical properties and durability as well as availability and comparable low price.

The performance of concrete structures is significantly affected by crack formation. On the one hand, the crack formation is a fundamental and desired behavior of structural concrete which provides efficient structures. On the other hand, the deformation behavior of concrete can cause additional cracking which needs to be controlled in order to fulfill design criteria and to provide sustainable structures. Thus, crack assessment is an important task of structural engineering - especially if water permeability is requested. Common application cases are water retaining structures like sluices, tanks or dams as well as massive bridge foundations and even members with aesthetically requirements. Further implications arise since these structures are often very thick and large in scale. This refers to a deep understanding of the material properties and their development over time as well as to a deep understanding of complex stress states and the associated cracking.

It is the motivation of this thesis to develop a reasonable approach to assess the cracking patterns to be expected when designing large scale concrete structures. Therefore, a discrete cracking model is included in a 3D Finite Element model and applied for two practical cases.

1.1 State of the Art

1.1.1 General member behavior in the uncracked state

Concrete is a construction material characterized through continuous volume changes during its life time. It is casted in a fluid state but after setting it starts to harden. The hardening process is associated with exogenous chemical reactions, which change the temperature of the casted structural member significantly. With increasing thickness transient temperature fields occur. This transient temperature field consists of different components that can be broken down into constant, linear and non-linear parts, where the associated deformation behavior would be:

constant temperature component	→	axial deformation
linear temperature component	→	linearly distributed deformation (curvature)
non-linear temperature component	→	non-linearly distributed deformation

If this deformation behavior is restrained the resulting restraint stressing depends on the type of deformation that the member experiences and the restraint situation. In case of perfect restraint the associated stressing can be categorized accordingly:

axial strains	→	axial restraint force N_{rest}
linearly distributed strains	→	restraint moment M_{rest}
non-linearly distributed strains	→	eigenstresses

The interplay between imposed deformation, restraint situation and resulting stresses is exemplified in figure 1.1 on basis of the imposition of a constant temperature component. In case of axial restraint also a fully constant stress distribution occurs, however, additional bending stresses occur in case of restraining the member eccentrically.

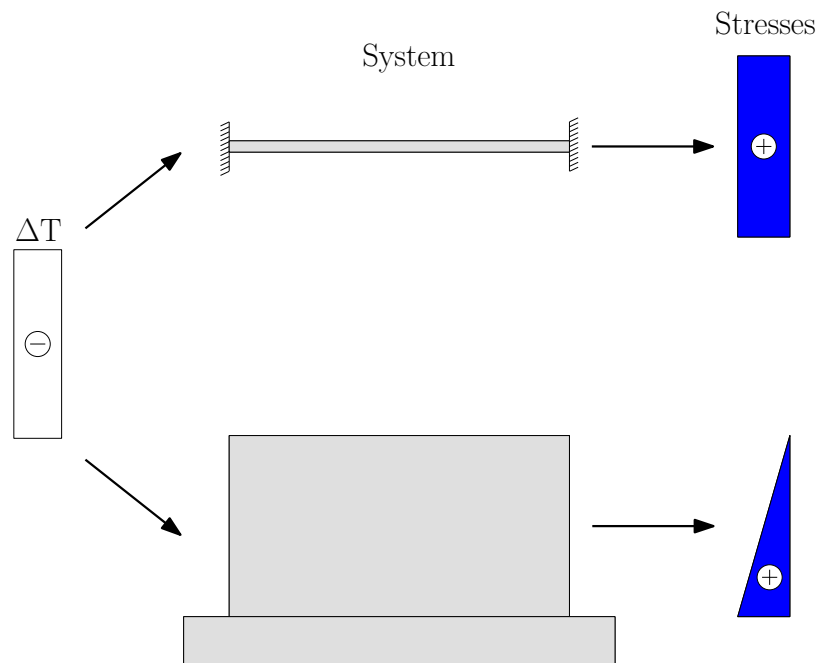


Figure 1.1: Stresses according to the restraint conditions

Another significant influence on the final stressing is the activation of self weight due to uplift of the member. As outlined in [4] this activation depends strongly on the activated member length. For the purpose of illustration, figure 1.2 exemplifies this effect with the typical case *wall on foundation*.

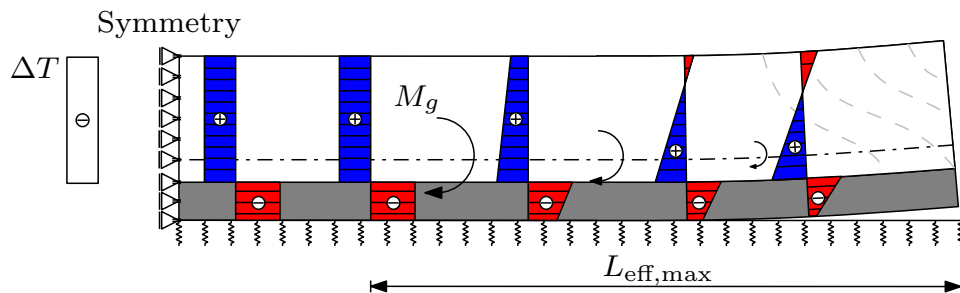


Figure 1.2: Stress distribution over the height of a wall according to the self weight activation along the member length taken from [4]

Permanent stressing causes additional strains to concrete members. These stress-dependent volume changes, characterized by the viscoelasticity of concrete, are, in civil engineering, described through creep and relaxation. This viscoelastic behavior is time dependent and affects the overall stress state of the member during its lifetime. Since this thesis focuses on restrained members at an early age, viscoelastic effects were taken into account through the whole simulation. Especially in restrained systems in which the stress state is closely tied to any imposed strain on the member, it is necessary to correctly assess viscoelastic effects with respect to the present stresses. For the computational consideration of viscoelastic effects in hardening concrete different models exist. The simulations in this thesis were carried out on the deformation based approach given in [4].

1.1.2 Analytical prediction of crack formation on basis of stress distribution

For a targeted crack assessment, crack formation can be categorized as following:

Separating cracks, as shown in figure 1.3, are cracks that extend through the entire width of the member. Depending on the member, they do not necessarily have to proceed over the whole height. As long as these cracks propagate through the width they may provide critical leakage paths.

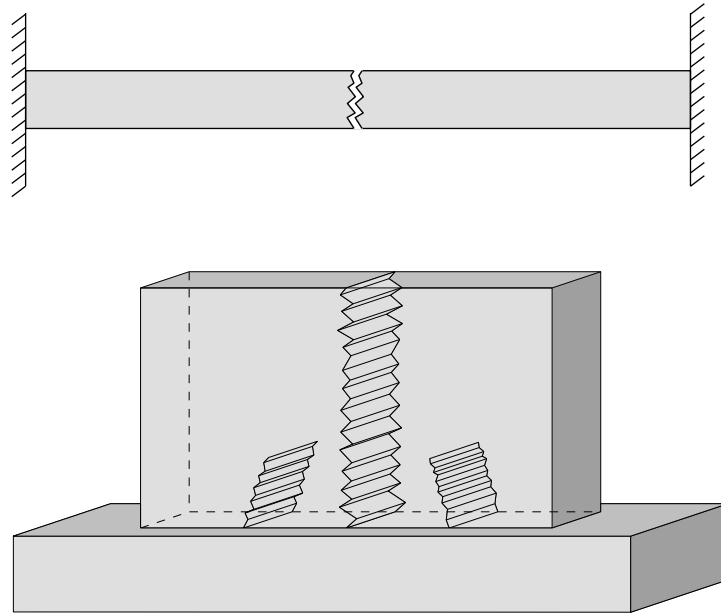


Figure 1.3: Separating crack in the case of a full restrained member and eccentric restrained member

Bending cracks do not proceed over the thickness and are strongly connected to a compression zone in the cross section. Bending cracks are usually caused by the restraining of curvature, e.g. in case of ground slabs with temperature gradients over the thickness restrained by self weight activation. Figure 1.4 exemplifies such case. It should be noted that the tightness of the structure can be provided by a minimum thickness of the remaining compression zone along the whole length of the crack, however, bending cracks are usually the starting point of separating cracks in case of additional axial stressing.

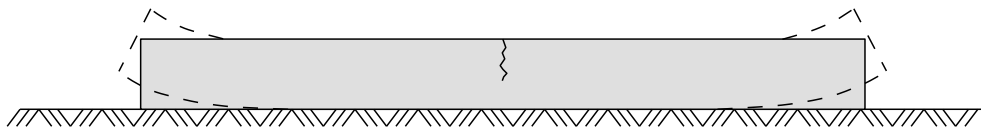


Figure 1.4: Separating crack in the case of a full restrained member and eccentric restrained member

Surface cracks and local cracking in the interior present a rather peculiar case of concrete cracking, since the driving forces behind the cracks are solely based on eigenstresses and their changes over time. In the early stages while the member is heating up due to hydration heat whereas the surface remains cold since it is exposed to the environment, as seen in figure 1.5, surface cracks start to form while the core is still expanding and

under compression. This effect can be increased by additional drying shrinkage of the exposed surface area. Later, the core cools down again and the eigenstresses will be reversed. Possible surface cracks will be partly closed and the core can even experience tensile stresses which in turn causes localized interior cracking.

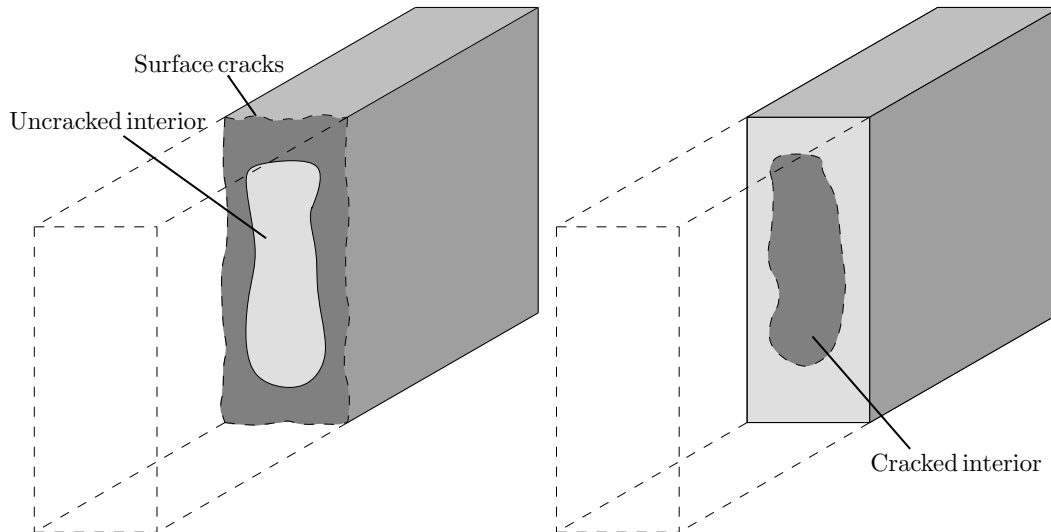


Figure 1.5: Crack formation due to eigenstresses; **left:** early cracking at the surface; **right:** local interior cracking at temperature equalization

The analytical prediction of crack formation on basis of the stress distribution refers to the check of a crack criteria. A common approach is the comparison of maximum tensile stresses with the present tensile strength of the material, the so-called cracking index. This comparison takes place on the basis of absolute state variables for selected material points in the cross-section. However, with increasing structural member thickness, the stress fields of a cross-section overlap with significant eigenstresses. An engineering approach for the specific distinction of the type of cracking to be expected with special regard to the existing eigenstresses in the stress field is proposed in [6] or [8]. Here, the risk of cracking is assessed with the so-called "macrocrack index". In detail, the stress maxima including eigenstresses are compared with 80% of the lower limit of tensile strength ($0.8 \cdot f_{ctk,0.05}$). If these existing stresses exceed this criteria, it is assumed on the conservative side that the eigenstresses are completely reduced through microcracks or localized crack formation. Subsequently, the stress distribution without eigenstresses is now compared with the average tensile strength f_{ctm} . If these stresses exceed also this criterion, sufficient energy can be assumed to exist in the cross section in order to cause a macrocrack in the following.

1.2 Motivation and objectives

The objective of this thesis is the development of a discrete cracking model and its implementation in a 3D Finite Element model. This model should enable numerical

investigations on the interplay between restraint stressing and cracking to be expected with distinct considerations of stress resultants and eigenstresses in regard to macrocrack formation and surface cracks. The applicability as well as a tentative validation shall be provided by the simulation and analysis of two practical cases.

1.3 General approach

This thesis is set up on volumetric FE models for time-discrete simulations of hardening induced restraint stressing in the uncracked state. Usually the models are designed with the usage of symmetry conditions, as shown in figure 1.6.

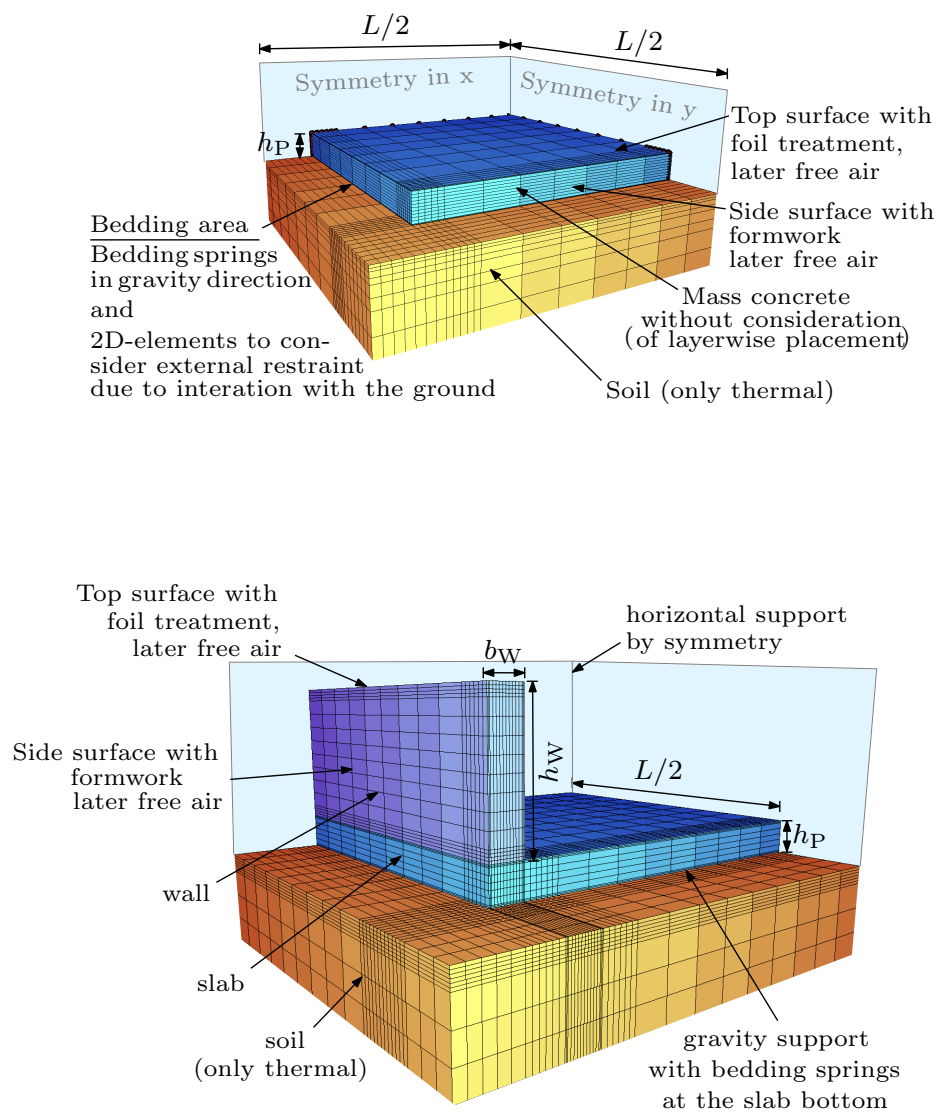


Figure 1.6: Possible 3D models of restrained systems and considerations for symmetry

In a second step, a model for discrete cracking is implemented in the most stressed cross section in the plane of symmetry. The cracking is then simulated only in this cross section at a single point of time which was identified to be decisive.

2 Relevant material behavior and its computational consideration

2.1 Thermo-mechanical behavior of hardening concrete

2.1.1 Preliminary remarks

The thermo-mechanical behavior of hardening concrete was simulated in the following studies by time step-based FEM simulations. The applied material model was taken from [4] without significant modifications, however, shrinkage was neglected at this stage. The neglect of shrinkage in the present study is justified by a focus on general cases dominated by thermal gradients, whereas shrinkage is of minor importance. Of course, in reality special cases with significant influence of shrinkage exist and require further investigations. Altogether, the aim of the present study (general understanding of crack formation when critical stress states are reached) is not affected by this engineering assumption.

A general presentation of the simulated material behavior and the functionality of the applied material model is given in the following.

2.1.2 Maturity, heat release and evolution of thermal properties

The hardening of concrete is an exothermal process. Initially, fresh concrete has a certain temperature, depending on initial temperature of aggregates and water as well as occurring heat in the mixing process and additional influences due to environmental conditions of the surrounding. In the following the exogenous chemical reaction of hydration causes a heat release. Hereby, the process speed depends on the temperature of the concrete itself. This effect can be described by the maturity method of [3].

The absolute temperature reached in the member depends significantly on the type and amount of cement used as well as the thickness of casted member. The influence of the latter is mainly caused by a limited thermal conductivity of concrete. This limited thermal conductivity restricts the outflow of heat from the interior of the member which in turn causes it to warm up even more. The thermal conductivity of conventional concrete decreases with proceeding hydration by 30% which can be considered in thermal analysis on basis of the hydration progress. The heat storage capacity shows also changes in reality,

however, this effect can be included in the heat release function so that the computationally considered heat storage capacity can be implemented as constant over time.

2.1.3 Evolution of mechanical properties

In the hardening process concrete undergoes a significant change of mechanical properties depending on the concrete age. Fresh concrete has almost no mechanical values, however, after setting the evolution of Young's modulus, compressive and tensile strength begins. The evolution of mechanical properties is coupled to the aforementioned thermal processes. Properties like Poisson ratio μ and temperature expansion coefficient α_T shows also significant dependencies in the course of hardening, however, after setting they can be assumed as constant.

Next to this, concrete is characterized by additional volume changes by time. These volume changes are independent as well as dependent on the stress state. In general, stress-independent volume changes occur due to shrinkage caused by hydration as well as drying. The stress-dependent volume changes occur due to viscoelasticity.

The simulation of viscoelastic effects in hardening concrete is a challenging task. Main reason is the significant dependency of the viscoelastic behavior on time. This refers to both the influence of the age of concrete at loading as well as the fact that viscoelastic strains occur only in the course of time. In the simulations of this thesis a conventional solution on basis of discrete superposition of viscoelastic strain increments with respect to the viscoelastic potential of each stress change in each time step was applied. Further information can be found in [5].

2.1.4 Coupling and material model for computational purposes

A time discrete coupling of thermal and mechanical behavior of the hardening concrete is essential for realistic results. This coupling was achieved by simulating the evolution of each relevant material property from the effective concrete age. This effective concrete age is a state variable in each element and represents the individual concrete age of each element with regard to its specific maturity.

2.2 Behaviour under tension

In this thesis, tensile behavior of concrete is derived from the material models given in the Model Code 2010. Since tensile failure is a discrete phenomenon, this approach considers concrete in two separate states: (i) uncracked state and (ii) cracking. For the uncracked state the bilinear stress-strain relation is applied in order to represent the softening behavior of concrete adequately. As soon as cracking occurs, the behavior will be derived on basis of the fracture energy.

2.2.1 Stress-strain relation in the uncracked state

The bilinear stress-strain relation considered in this study is shown in figure 2.1. The first section (I) presents the linear elastic behavior with a Young's modulus of $E_{c,28}$, whereby the concrete is assumed to be fully undamaged. The second section (II), occurs at a stress level above $\approx 90\%$ of the average tensile strength of concrete (f_{ctm}). In this stress state the microcracking of concrete increases significantly and leads to a distinct softening.

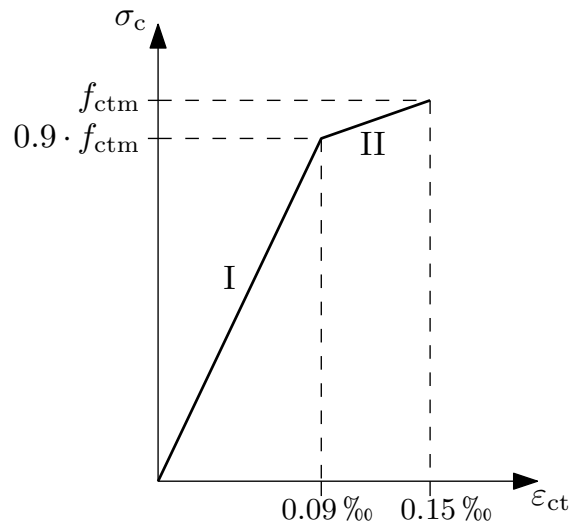


Figure 2.1: Stress-strain diagram for uncracked concrete

In this state, the concrete behavior can be assessed on basis of strains. A further definition of a fracture zone would not be required.

2.2.2 Crack opening and fracture energy

As soon as the tensile strain exceeds the ultimate strain, which occurs at the level of f_{ctm} , the microcracks start to grow into each other and form a macrocrack with an arbitrary crack opening w . The physically occurring crack width is a result of the localisation of tensile strains in the vicinity of the macrocrack as well as the size of the area affected by the crack. This localisation is the reason why the material behavior after exceeding the ultimate strain needs to be defined on basis of the crack width.

Figure 2.2 shows a common bilinear stress-crack width relation for cracking concrete. It shows that concrete is still able to transfer tensile stresses over a crack even though its maximal tensile strength was reached. This property of concrete is also known as softening behavior. A rule of thumb is that this effect can be observed for crack widths smaller than 0.1 mm, however, it becomes less relevant with further crack width progression.

From physical perspective, this behavior can be described with the fracture energy required

to fully open the crack. This fracture energy G_F corresponds to the area under the stress-crack opening relation.

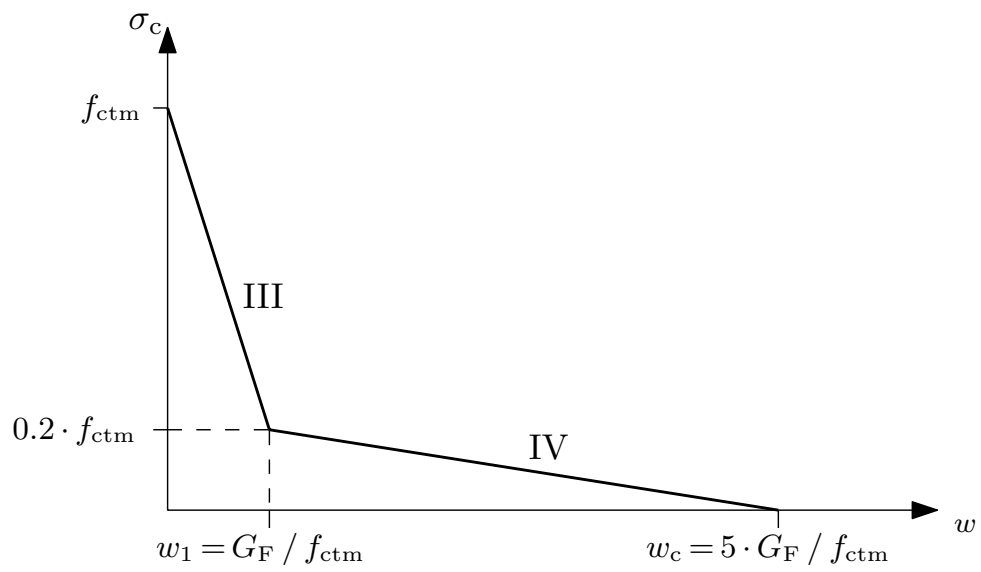


Figure 2.2: Stress-crack opening diagram

3 Discrete crack modeling

3.1 General remarks

Discrete crack modeling in selected cross sections is the first step for macrocrack simulation. In contrast to integrated solutions, which would enable possible crack formation everywhere in the structure, such approach requires the prior definition of the cross section in which cracking can occur. All other parts of the structure remain uncracked. Of course, such procedure is subject to a reasonable definition of the cross section with cracking and requires also a critical interpretation of the effect of linear-elastic behavior outside the crack, however, such procedure excludes also uncertainties from overdetermined calculation models and enables relative robust non-linear calculations.

In order to get realistic results it is necessary to model localised concrete failure in the prior selected cross sections without diminishing the mechanical properties of the rest of the concrete member. Besides, the localised concrete failure in the prior selected cross section needs to represent the softening with respect to the affected areas in the vicinity of the macrocrack. According to [1] and [7] the correct assessment of tension stiffening and softening behavior will have a significant impact on crack propagation. Modeling strategies which do not include softening, such as the "element cut-off" model shown in 3.2.1, represent therefore always a "worst case scenario".

In this thesis discrete cracks were only simulated in the symmetry axes of the member, as shown in figure 1.6. This approach was derived from the findings in [4] and [1] since that is the cross section with the highest risk of macrocrack formation.

The implementation of the failure elements in the cross section of symmetry was achieved by non-linear springs in each of its nodes. In the uncracked state, these springs represent the symmetry condition. As soon as the spring force exceed 90% of the average tensile strength of concrete (f_{ctm}), softening and crack opening follow. In order to accomplish this, the stress-strain relation of figure 2.1 was modified in section (I) in order to ensure the correct implementation of symmetry. The outcome of this thought process is depicted in figure 3.1. In detail, the very high stiffness in the new section (I') ensures a plane cross section at the plane of symmetry. After exceeding 90% of the average tensile strength of concrete (f_{ctm}) the continuing stress strain relation in (II) enables the discussed softening through microcracks before localisation in a discrete crack.

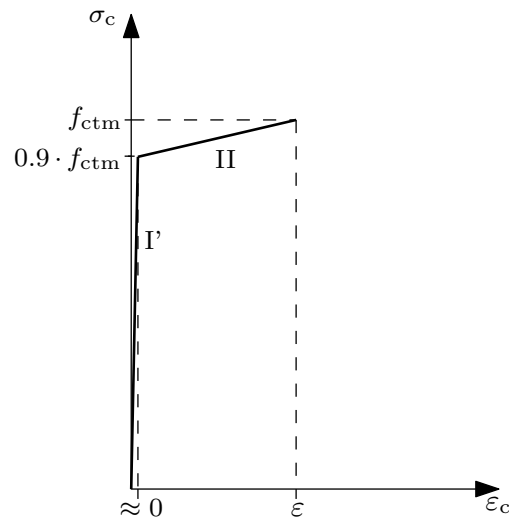


Figure 3.1: Modified stress-strain relation for spring elements used in the plane of symmetry with special regard to softening before macrocrack formation

This stress-strain relation in the uncracked state can be combined further on with the stress-crack opening relation. Since the implementation in the calculation model was achieved by springs the final stress-strain and stress-crack opening relation had to be transferred to a stress-displacement relation. This definition required a reasonable size of the localisation zone for section (II) of the uncracked state. In a first assumption this localisation zone was defined with respect to the geometrically set distance of primary cracks according to [4].

In the case studies of this thesis two different approaches for the stress-crack opening relation were investigated. The final stress-displacement relations for the springs are presented in the following.

3.2 Applied approaches

3.2.1 "Element cut-off" without softening

The first stress-displacement relation considered in this study was a pure symmetry condition without any softening, neither before reaching the tensile strength f_{ctm} nor afterwards. It is also known as the "element cut-off"-model and the underlying stress-displacement relation of the springs is depicted in figure 3.2. In detail, it emulates the symmetry condition where the cross section is kept plane, but with the possibility of fully unrestrained nodal displacements as soon as the stress level of f_{ctm} is reached. Through the failure of

individual springs, localized cracking occurs and thus a stress redistribution starts to take place. This in turn causes more springs to fail until an equilibrium is found.

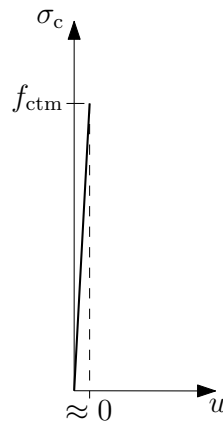


Figure 3.2: "Element cut-off" relation for spring elements used in the plane of symmetry

Of course, without the possibility of any softening this model shows the highest stress redistribution when the stress level of f_{ctm} is reached initially, however, in terms of crack propagation this model has to be seen as a "worst case scenario". This theoretical approach gives a starting example for the comparison with approaches including softening behavior in order to determine this influence.

3.2.2 Softening fracture

The second stress-displacement relation considered in this study was a pure symmetry condition in the linear elastic section of the uncracked state (I'). After a stress level above $\approx 90\%$ of the tensile strength of concrete (f_{ctm}) is reached, the stress-displacement relation simulates softening in the uncracked state according to [2] until a stress level of f_{ctm} is build up. After exceeding the uncracked state the stress-displacement relation simulates softening in the uncracked state according to [2]. This means the springs continue to take a part of the acting forces even though the concrete exceeded the ultimate strain and crack opening starts.

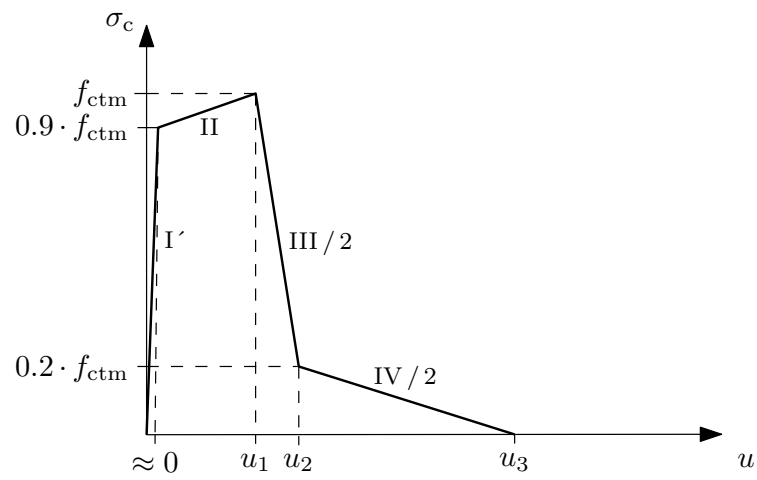


Figure 3.3: Combined stress-strain relation for spring elements used in the plane of symmetry with special regard to softening before and during macrocrack formation

4 Case study

4.1 General remarks

The following case study is based on numeric simulations of volumetric models created with the finite-element software SOFiSTiK. In detail, the mesh was generated with the module SOFiMSHA for regular meshes, the temperature field due to hydration was simulated with HYDRA and resulting stresses were finally determined with ASE. The 3D simulation was necessary since the temperature field is strongly influenced by the member thickness while the resulting forces are dependent on the member length. The models were created by using symmetry, as illustrated in 1.3. The symmetry condition is fulfilled by using springs in the symmetry planes with stress-strain relations as introduced in 3.2.1 and 3.2.2.

The presented macrocrack model was applied in the simulation of two distinct types of restrained members: (i) a large foundation with small external restraint and (ii) a wall on foundation with significant external restraint.

The simulations are time-step based, whereby the time-step length is adjusted during the simulations to minimize the computational effort. In time frames where significant changes occur quickly (e.g. the initial temperature increase of the just casted concrete) the time-step was set to 1 hour. By time these changes smoothen in the process (e.g. temperature increments are significant smaller in a short time-step) therefore the time-step is set to be larger (up to 12 hours in the end).

The 3D calculation models consist of linear elastic volume elements with an integrated thermomechanical material model according to [4]. The herewith simulated material properties of the concrete comply in both cases with a reference concrete which represent normal strength concrete C35/45 with 300 kg of CEM III A. The material model recreates the hydration induced temperature development as well as the development of the material properties. Simultaneously, parallel volume changes as a result of viscoelasticity are considered. It should be noted that the thermomechanical material model was implemented in each element individually giving each element its own aging.

4.2 Large concrete foundation

4.2.1 Specifications of the example

Figure 4.1 illustrates the finite element model for the large concrete foundation. It represents a very large concrete block with very large dimensions. Such members are predominantly build as bridge piers in rivers, e.g. for the New Botlek Bridge in The Netherlands [9]. In reality the casting process consists of pouring in layers and lasts several days in total. Maximum temperature in the member and temperature distribution is thus influenced by a delayed heat release of the subsequent layers. Besides, environmental conditions in the construction process, e.g. underwater concrete placement, can have significant influences in addition.

In contrast to the mentioned example of the New Botlek Bridge, this study refers to a theoretical case whereby the casting process was simulated in a single step to obtain the worst case scenario in terms of maximum temperature and maximum temperature gradients. Also, the block was simulated above ground in formwork and surrounded by air, whereby the formwork was removed after 72 hours. The vertical bedding of the block was simulated with nonlinear bedding springs. These spring solely work under compression in order to simulate the interaction between temperature-induced curvature and self weight activation (lift off of the edges of the structure due to temperature changes). However, there are additional volumetric elements for the soil considered in the model in order to represent the heat insulation effect at the bottom of the block.

The thermal boundary conditions at the free surfaces are characterized through convection taking into account the formwork, the environmental temperature and wind. After stripping the respective heat transfer coefficient on the free surfaces are adjusted according to a pure concrete surface. The thermal boundary condition at the contact surface between concrete and soil is characterized by the heat flow between the neighboring elements. A detailed description of the heat transfer coefficients used in this thesis can be found in [4] while the system itself as well as the dimensions are shown in figure 4.1.

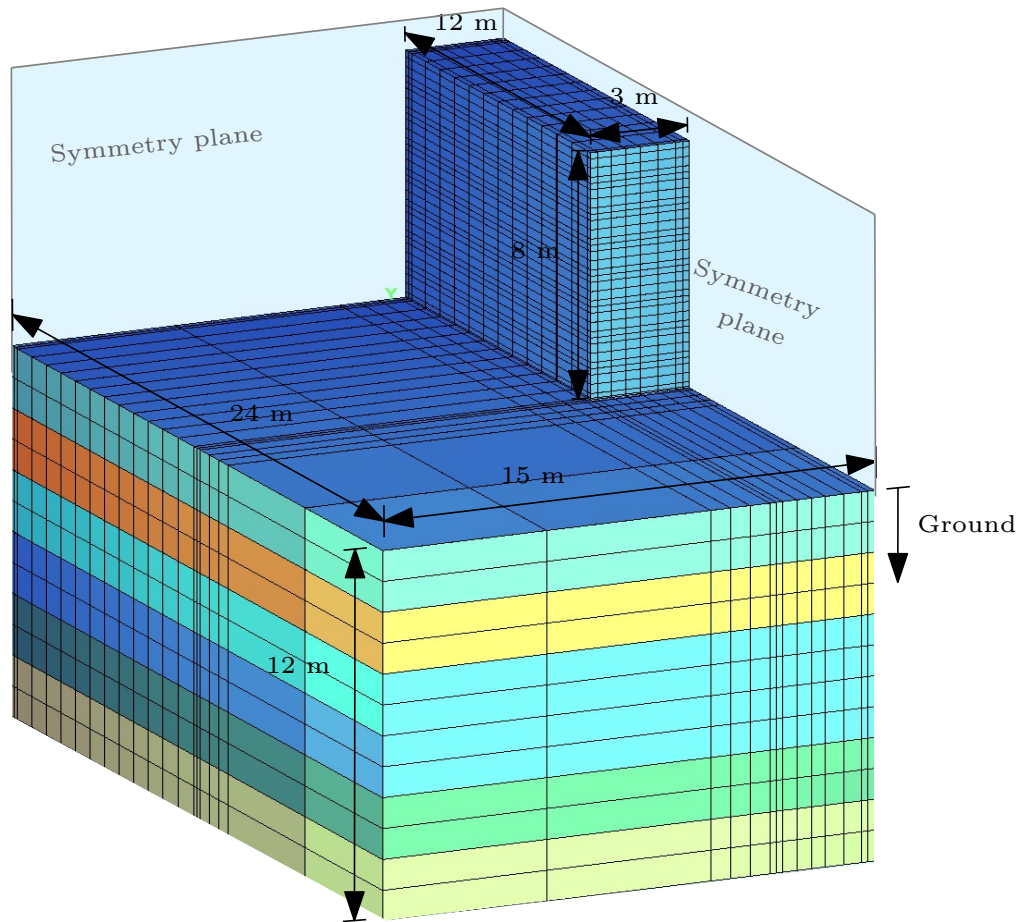


Figure 4.1: 3D model and dimensions of large concrete foundation

4.2.2 Calculation model

Figure 4.2 illustrates the volumetric calculation system with respect to the symmetry planes. The block is simulated through double symmetry which in turn reduces the element number while achieving same results. The symmetry conditions are implemented through springs. These springs were further used to investigate the possibility of transversal and longitudinal concrete failure in the critical point of time.

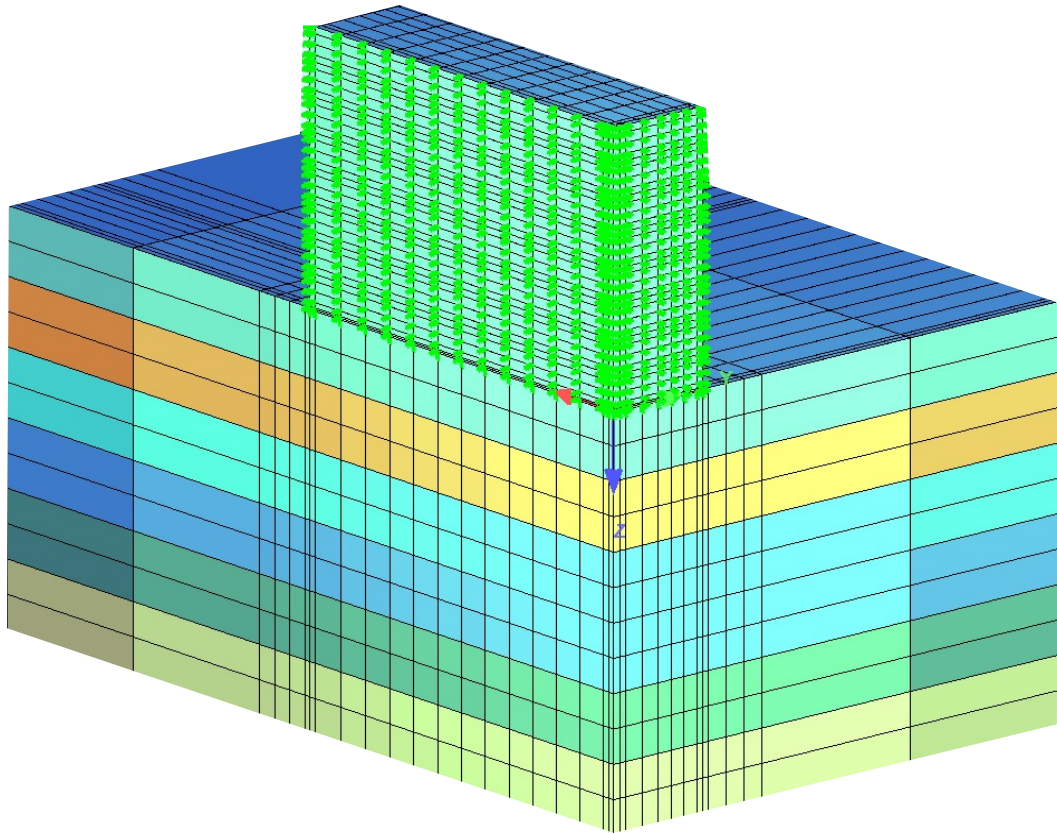


Figure 4.2: Implementation of symmetry planes on concrete block

4.2.3 Hardening-induced temperature and stress history

The concrete block starts out with a fresh concrete temperature of 23 °C while its bottom surface is slightly cooler at 17 °C. This is due to the cooler adjacent ground which immediately influences the temperature field of the block. By the following hydration and according heat release the block warms up. Considering the low heat transfer coefficient of concrete, the interior of the concrete block warms up the most and reaches around 62 °C. The maximum temperature increase of around 39 °C corresponds to nearly adiabatic boundary conditions. On the contrary, the temperature at the surfaces remains at any time below 40 °C. Figure 4.3 gives a general impression of this irregular temperature distribution of the cross section at the time of temperature maximum in the interior.

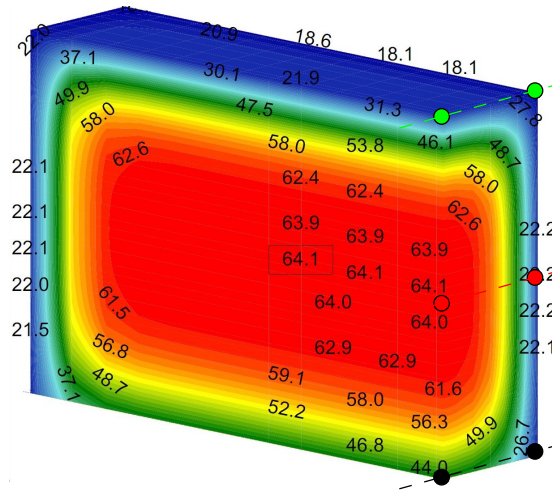
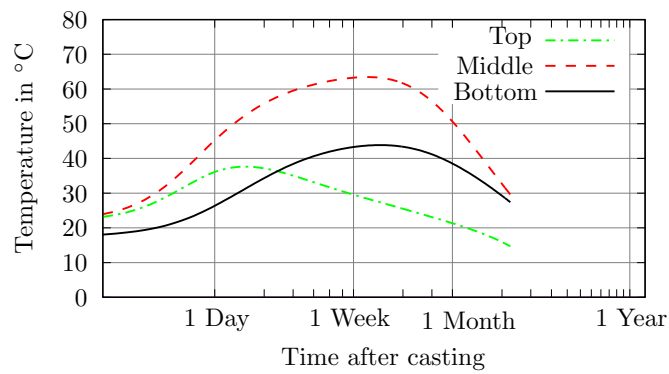
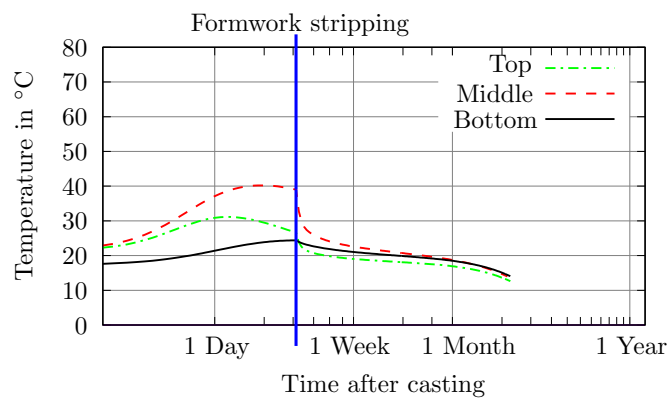


Figure 4.3: Determined maximum temperature distribution in °C at $t = 192$ h

For the purpose of illustrating the history of this irregular temperature development in the cross section, the temperature development is shown in figure 4.4 for 6 selected points.



(a)
Three different points over the height in the interior of the block

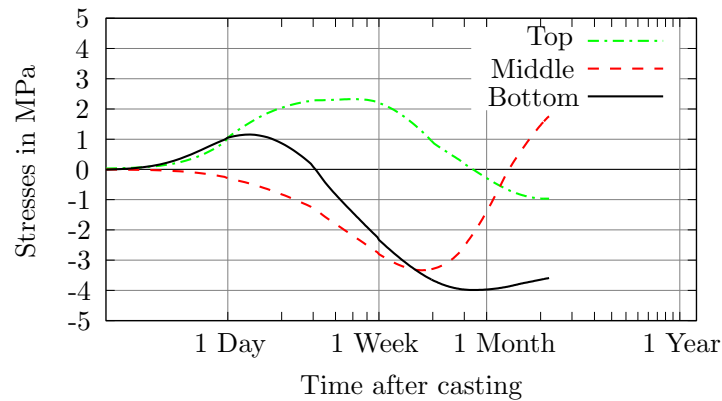


(b)
Three different points over the height on the surface of the block

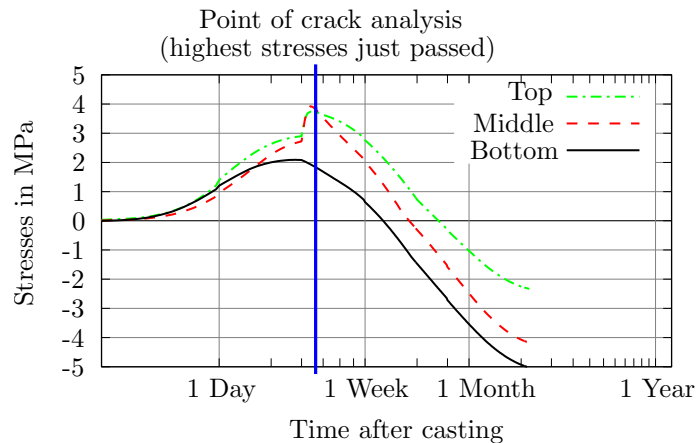
Figure 4.4: Temperature history in selected points in the cross section of longitudinal symmetry

The according stress development of the same material points as in 4.4 is given in 4.5. Figure 4.5 shows normal stresses (σ_x) of the global axis x , which is parallel to the longitudinal axis of the body. The overall highest tensile stresses form at the surface of the block with an slight additional increase for a short period of time after formwork stripping.

Furthermore, these stress histories indicate a significant non-linear stress distribution with an almost revers proportionality of stresses in the interior and the surface zones. Due to significant warming up and imposed expansion of the interior whereby surface zones remain at the same time on a significant lower temperature level a distinct interaction in the cross section is caused: the surface zones were set under tension while the interior of the block is under compression. Such behavior is likely for members with very low external restraint and according to this also very small constantly distributed parts in the stress distribution.



(a)
Stress development in three different points on the longitudinal symmetry plane



(b)
Stress development in three different points on the surface of the block

Figure 4.5: Time based stress development of the block

For the aimed crack analysis of this member the stress distribution at 90 hours after casting was chosen. This stress distribution contains the highest tensile stresses as well as the

highest stress gradient between interior and surface zone. All further analyses on crack assessments for the block were based on this stress distribution at 90 hours after casting, whereby cracking is to be expected since maximum tensile stresses exceed the present tensile strength.

The distribution of longitudinal and transverse stresses at 90 hours is the shown in figure 4.6. The highest stresses occur in the symmetry sections which will be analyzed with respect to crack formation further on. It should be noted that the transverse tensile stresses are higher than the longitudinal ones, however,

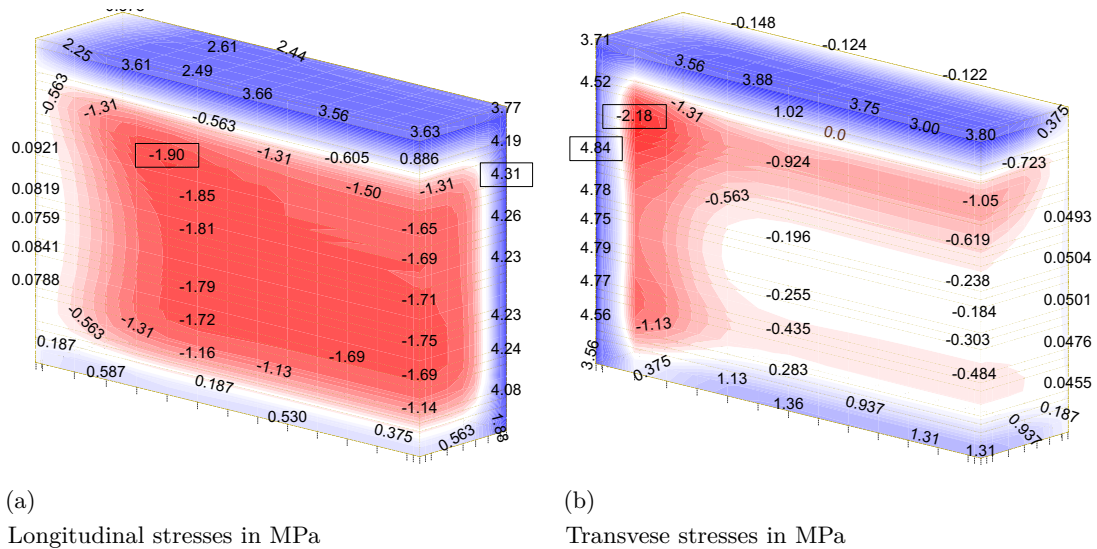


Figure 4.6: Simulation results: distribution of temperature and axial stresses at time of crack analysis ($t = 90$ h)

4.2.4 Influence of soil stiffness

In general, the insulation effect of the soil causes a temperature gradient over the height of the member. As shown in figure 4.7 the temperature field of the considered block shows a linear gradient over the height of approx. $2\text{ }^{\circ}\text{C}/\text{m}$.

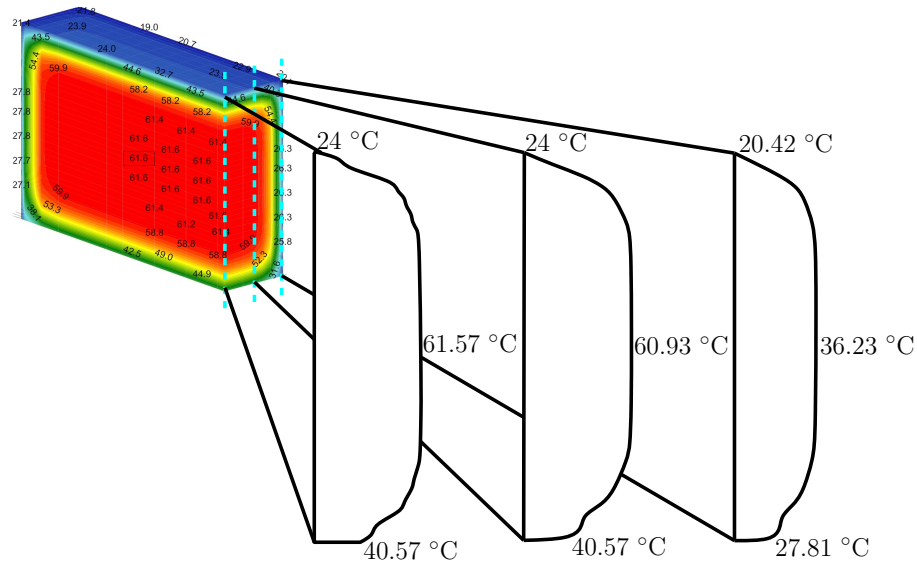


Figure 4.7: Temperature distribution over the block height in different cuts over the width at time of max. temperature ($t=90h$)

With increasing longitudinal dimension this cross sectional curvature causes a self-weight activation. However, the resulting bending stresses depend also on the vertical soil stiffness. This effect was investigated for the present block by a parametric study of the effect of soil stiffness on the occurring bending stresses due to linear temperature gradient.

Figure 4.11 shows the result. The correlation between bending stresses and soil stiffness in the symmetry plane is obvious, however, the absolute size of the stress change is very small in comparison to the magnitude of total stresses. The reason is the small length-to-height-ratio so that the possible self-weight activation is also very small. Overall, this effect is not of crucial importance for the final result.

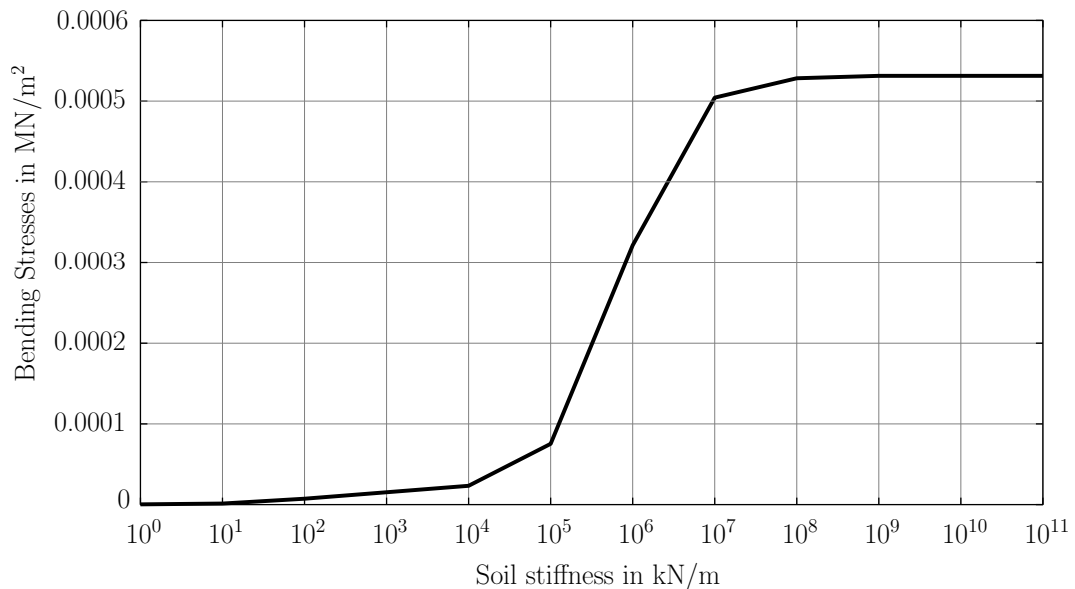


Figure 4.8: Soil stiffness influence

4.2.5 Discrete crack analysis with "element cut-off" approach

After determining the crucial point in time with the most critical stresses, cracking is simulated. In detail, the failure criteria of the spring is activated so that all springs with exceeding tensile stressing release energy. Altogether this causes a stress redistribution. For this section the springs were provided with the "element cut-off" stress strain relation which does not enable any softening, as explained in 3.2.1. The simulation for crack formation begins with the previously explained stress state and proceeds with abrupt spring failure upon reaching the failure criteria without additional transfer of stresses. This study conducted two types of simulations. At first spring failure was only initiated in one symmetry plane and then it was initiated in both symmetry planes. Figure 4.9 shows all the failed springs in the transverse symmetry plane. The crack pattern can be traced back through this illustration.

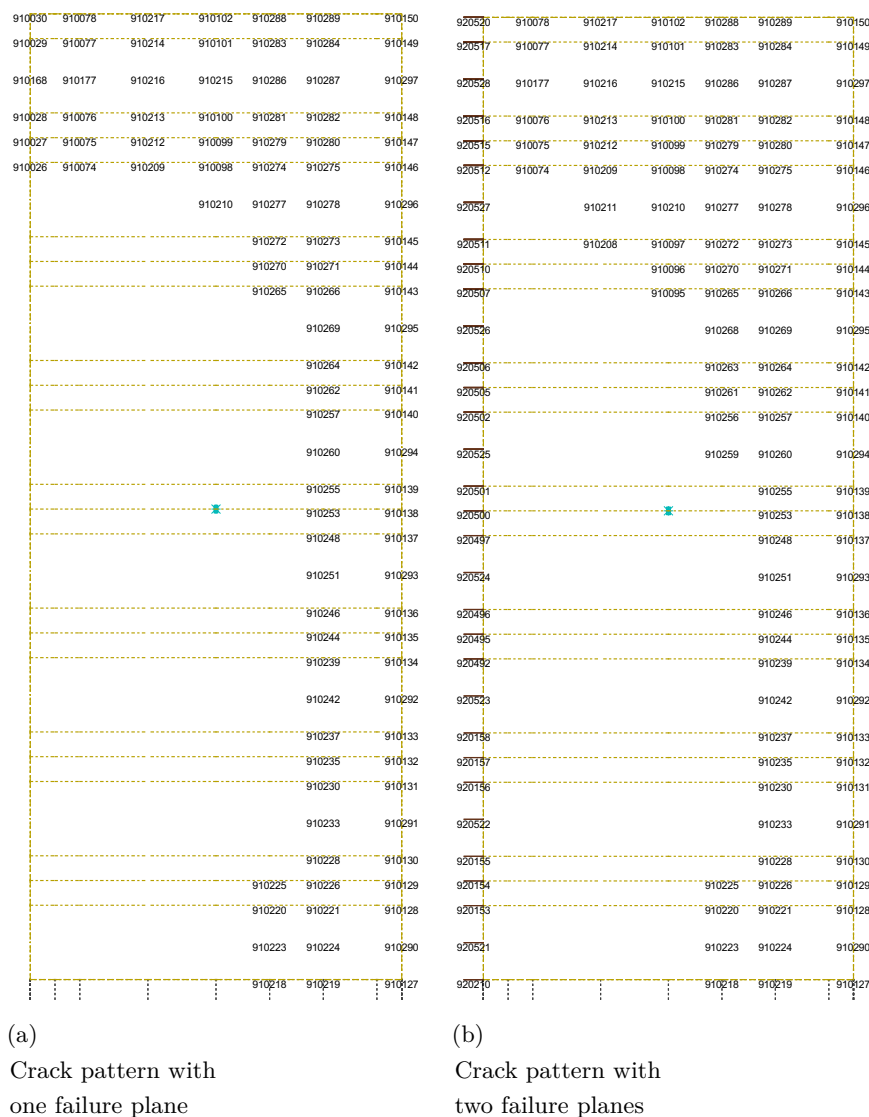


Figure 4.9: Comparison of crack patterns based on possible failure planes

Figure 4.10 shows the crack patterns for the two considered scenarios. The comparison of both results indicates that it is necessary to consider the combined action of both failure planes in order to ensure safe side conclusions.

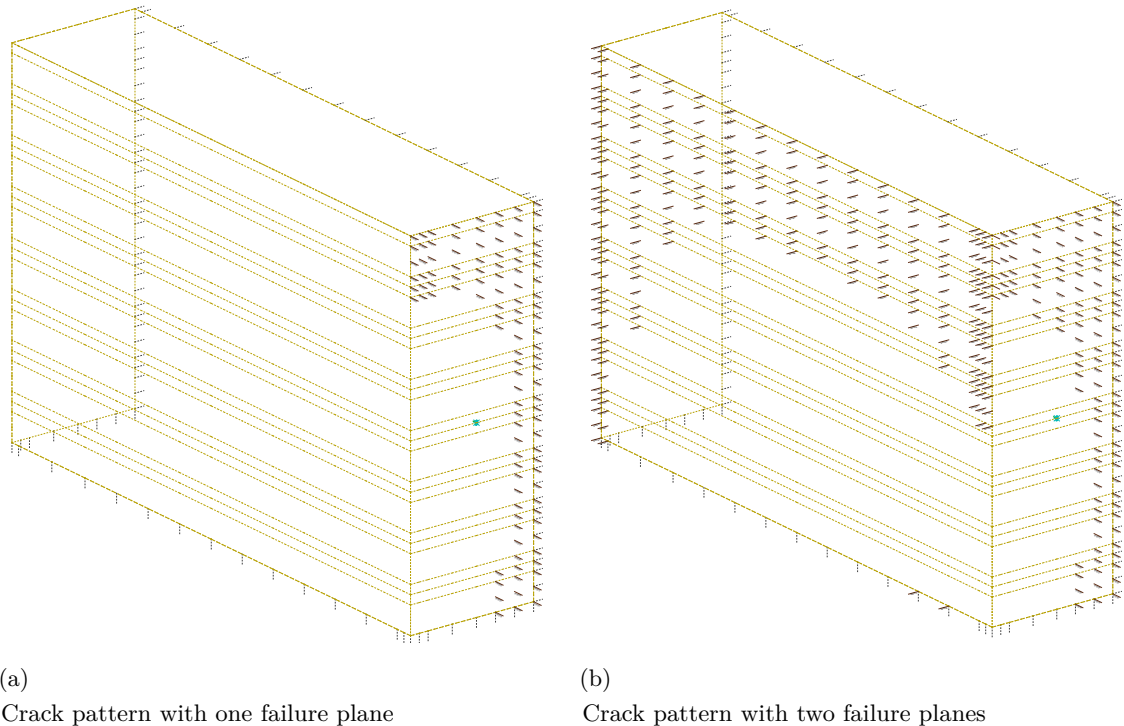


Figure 4.10: Comparison of crack patterns based on possible failure planes

4.2.6 Discrete crack analysis with softening approach

This section discusses the results of crack analysis for the investigated stress state but with enabled softening. This was achieved by providing the springs with a stress-displacement relation which includes softening, as explained in 3.2.2.

Figure 4.11 gives the nodal displacements for the planes of symmetry. As shown, only a few nodes that are close to the surface experience any displacements which in turn states that the intensity of cracking is very small. Although the crack criteria is reached, the possibility of tensile stress transfer of the failure plane with very small crack opening at the same time provides a significant relief from eigestresses. In the present case, an equilibrium can be found without the development of macrocracks.

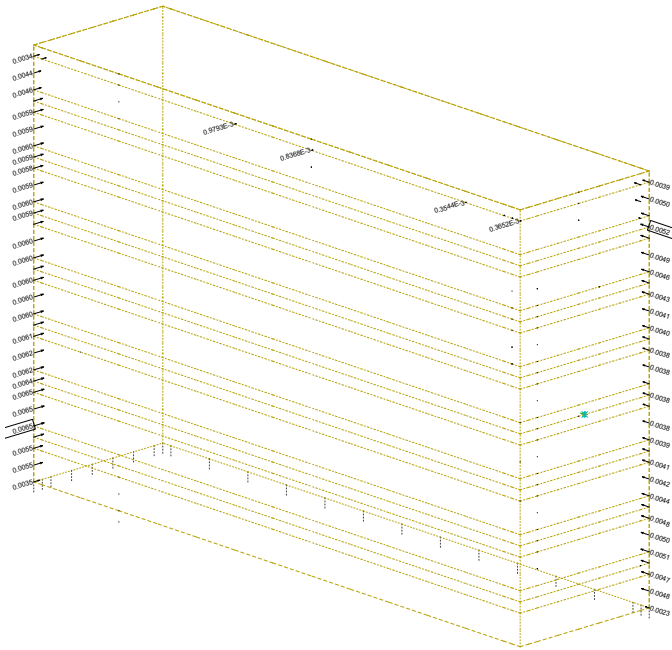


Figure 4.11: Crack pattern with two failure planes using softening approach

Besides, influences on the transversal crack pattern due to longitudinal cracking cannot be obtained as in the previous example. The reason is the insignificant cracking on the transversal symmetry plane, which hardly affects the stress state on the transverse symmetry plane.

4.3 Wall on foundation

4.3.1 Specification of the example

In this section the presented macrocrack model was applied in the simulation of members with significant external restraint. In detail, the typical case of a wall on foundation was investigated. Figure 4.12 illustrates the applied finite element model and its dimensions. The wall is casted on an already hardened concrete foundation, whereby the introduction of two symmetry planes refers to a centrally located wall on the foundation. The risk of cracking in the wall results from the later casting time of the wall and the herewith caused eccentric restraining by the foundation.

The present study starts with an already hardened foundation on the ground on which the wall is casted in a single step. Again, this neglects real site conditions, however, in case of the considered example this effect is of minor importance. Besides, the wall is also continuously kept in the formwork ignoring common construction site practice with earliest possible stripping. The vertical bedding of the system was simulated with nonlinear bedding springs below the foundation. These springs solely work under compression in

order to simulate the interaction between temperature-induced curvature and self-weight activation (lift off of the edges of the structure due to temperature changes and in this case also due to eccentric restraining at the wall bottom). Next to this, there are additional volumetric elements for the soil considered in the model in order to represent the heat insulation effect at the bottom of the foundation.

The thermal boundary conditions are characterized through the influence of the environmental temperature and the heat flow between concrete and soil in their contact surfaces. The heat transfer on the surfaces which are exposed to ambient air were simulated with a heat transfer coefficient of the surface including any effect of ambient temperature, wind and additional insulation due to formwork. The geometric dimensions of this model are based on [1] in order to provide comparisons of the determined crack patterns.

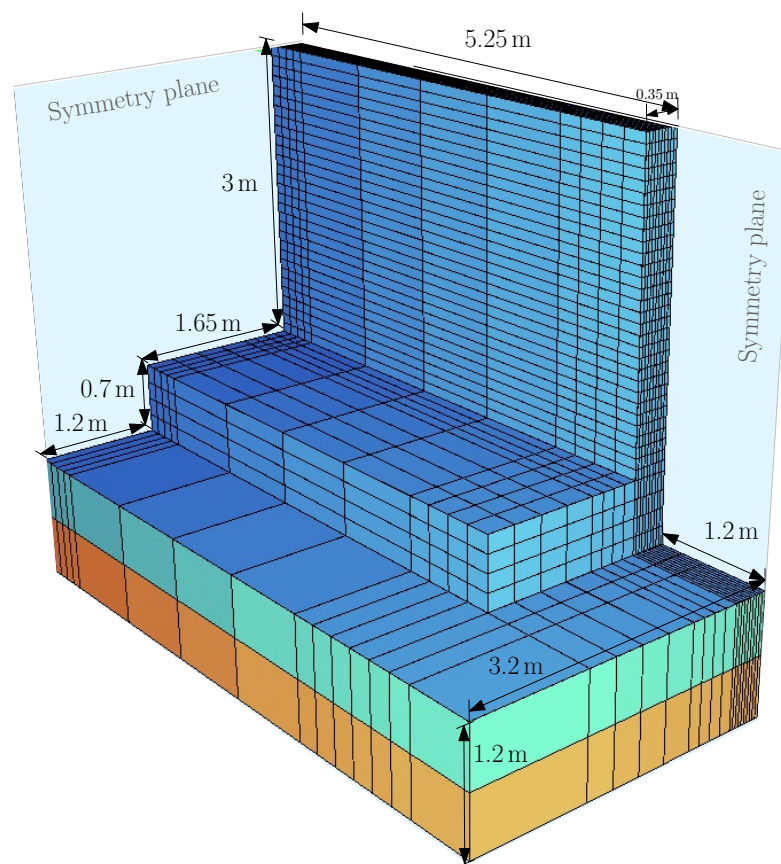


Figure 4.12: Dimensions and schematic representation of the engineering assumptions of the model

4.3.2 Calculation modell

Figure 4.13 illustrates the volumetric finite element model for calculation with respect to the symmetry planes. The member is also simulated through two planes of symmetry, a longitudinal and a transverse one. In the longitudinal direction the symmetry condition is again simulated with springs which will be used further for macrocrack simulation, however,

symmetry in transverse direction was simulated through rigid supports since cracking in longitudinal direction can be excluded by the limited width of the wall. It should be noted that the longitudinal symmetry condition in the foundation was simulated with rigid supports as well. This simplification is justified since the foundation is under high compressive stresses so that it is not likely that cracks will form there.

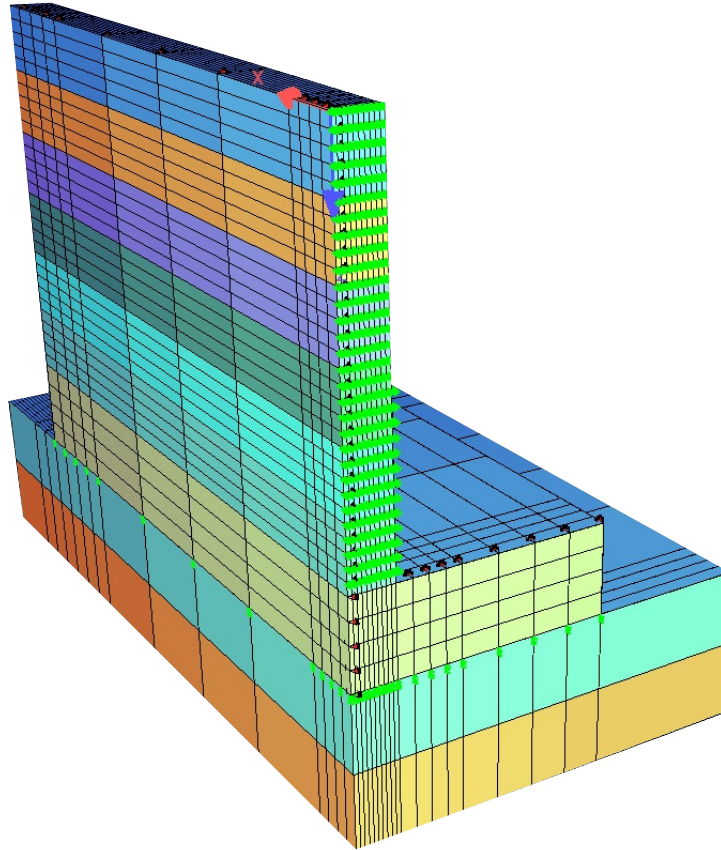


Figure 4.13: Calculation model of the simulated externally restrained member

During the simulations it was found that the FEM mesh requires a certain fineness over the width. This is due to the fact that the uncracked cross section contains significant eigenstresses, however, initial locally restricted failure at punctual stress peaks causes local stress redistributions. Since eigenstresses vary drastically over the width of the cross section, as shown in figure 4.14, a fine element partition over the width is needed to enable a realistic simulation of this local stress redistribution.

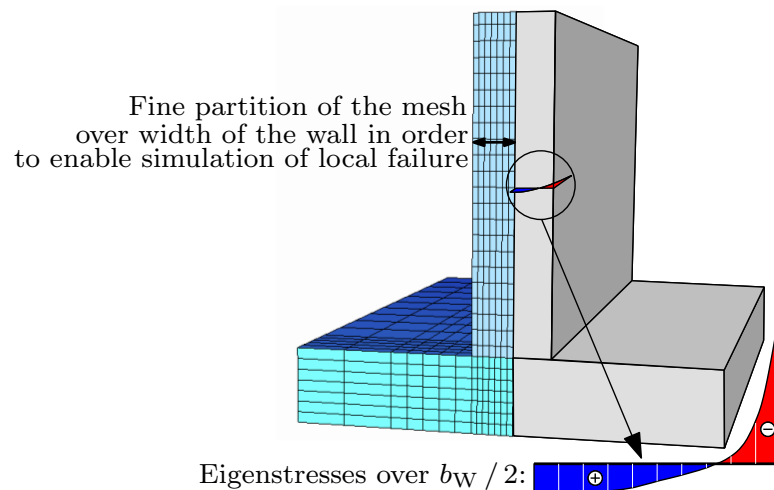
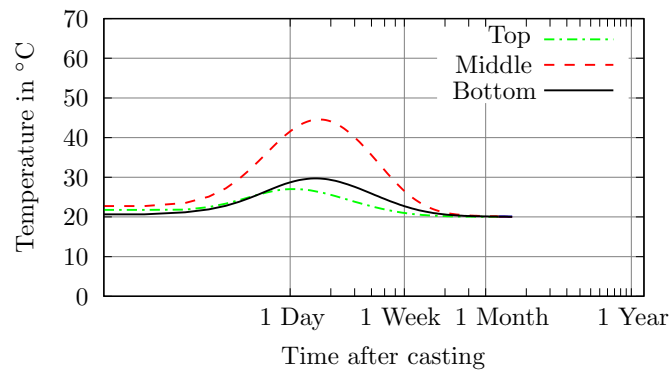


Figure 4.14: Symmetric illustration of the eigenstresses across the width of the member, green lines represent the chosen element width in which the stresses are recorded

4.3.3 Hardening induced temperature and stress history

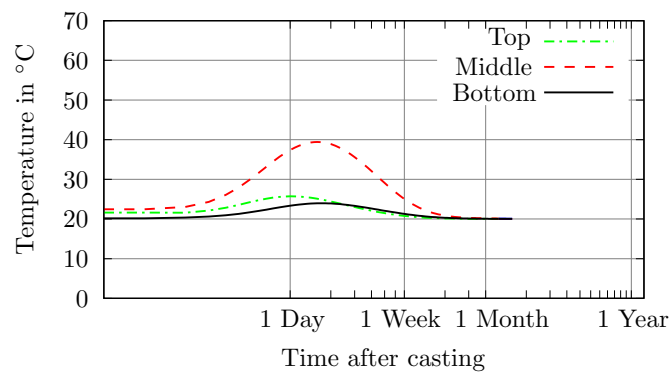
Analogous to the previous case, the temperature and stress history have been determined over an extended period of time. For the illustration of temperature and stress history over time, these parameters were shown for select points in the longitudinal symmetry section. This was done for the center of the wall width and the surface that is exposed to the environment. Longitudinal symmetry was selected since this section experiences the most stressing.

The temperature results for these points are illustrated in figure 4.4. The wall is kept in formwork over the whole period without any temperature shock and therefore the temperature development is smooth over time without any spontaneous drops. As expected, the first two days show the highest incremental changes in temperature. Besides, it should be noted that since the member is kept in its formwork the maximum core temperature reached the upper limit of maximum temperature to be expected in construction practice.



(a)

Temperature development in three different points on the longitudinal symmetry plane

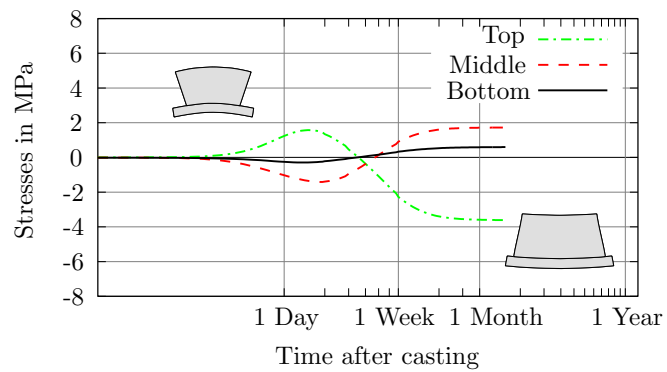


(b)

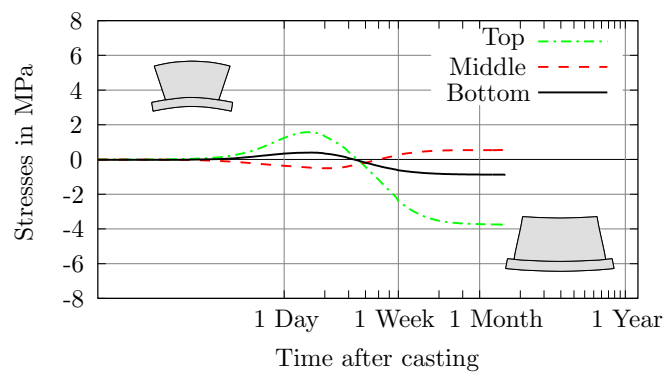
Temperature development in three different points on the outside of the wall

Figure 4.15: Time based temperature development of the block

Based on [1], the fresh concrete temperature for the casted wall is 25 °C. The wall shows also some initial temperature differences at casting since fresh concrete of the surface area is immediately affected by the ambient temperature. In comparison to the very thick block of the first example these differences are rather small. The simulation proceeds to cover a time frame of almost 2 months which upon review of the temperature development is sufficient since it covers the temperature peak and its equalization with the surrounding. From the point of view of stress assessment, this time frame is also sufficient since as long as temperature equalization is reached this time frame covers all necessary developments to describe early restraint behavior. Figure 4.16 illustrates the timely development of the longitudinal stresses (σ_x) in the plane of symmetry. At first since the wall expands due to increasing temperature it is held together from the stiff foundation, causing initial compressive stresses. When the wall starts to cool off, it contracts itself while this deformation is again restrained by the foundation. The deformation behavior is influenced by the evolution of the Young's modulus and viscoelasticity which finally leads to tensile stresses at equalization. Figure 4.16 enforces these statements and shows how the stresses shift from compressive to tensile stresses over the course of time.



(a)
Stress development in three different points on the longitudinal symmetry plane



(b)
Stress development in three different points on the outside of the block

Figure 4.16: Time based viscoelastic stress development of the block

The temperature field as well as the stress distribution in the cross section at 30 hours after casting is shown in figure 4.17. Both the temperature field as well as the associated stress distribution are strongly non-linear whereas tensile stresses at this state are restricted to the surface zones.

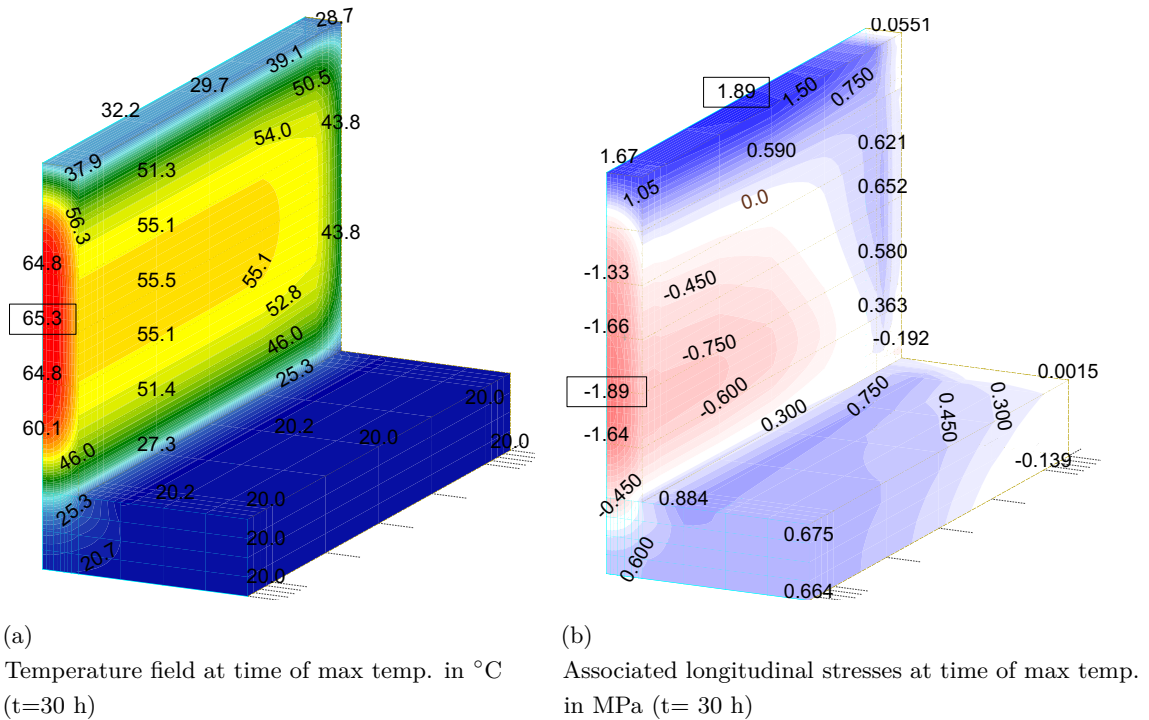


Figure 4.17: Simulation results: distribution of temperature and axial stresses

At temperature equalization ($t = 336$ h), the temperature field is almost constant whereas the stress distribution shows still a distinct non-linearity, however, tensile stresses are now dominant in the cross section, see figure 4.18.

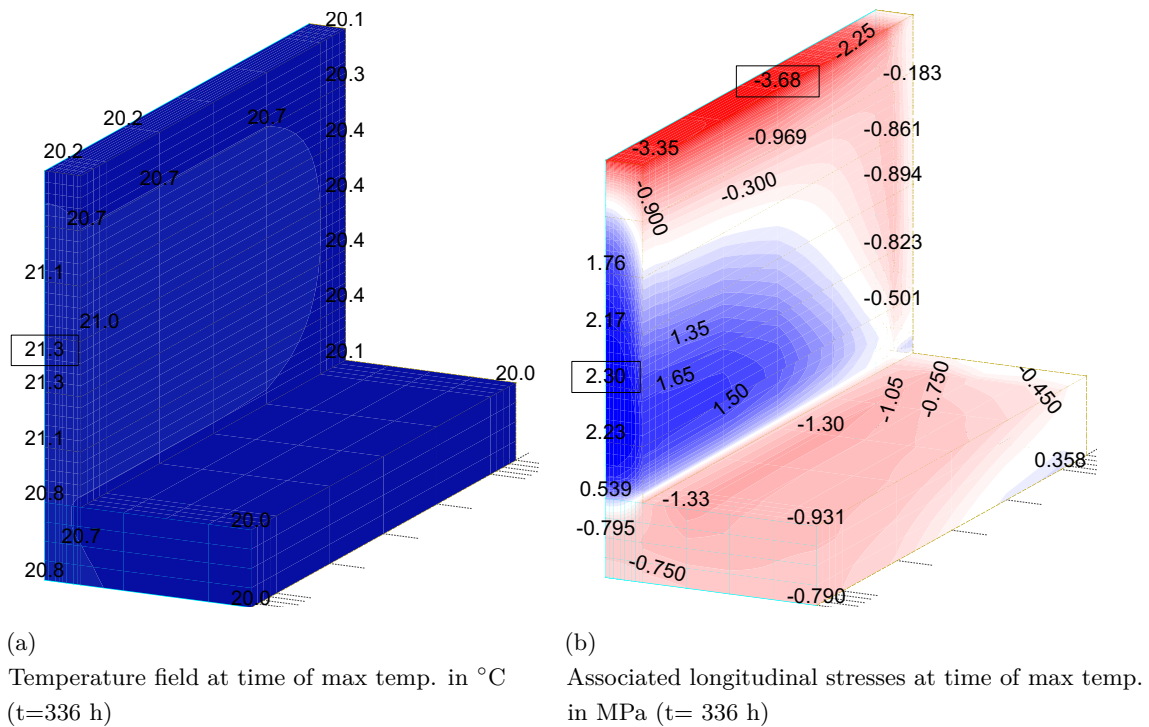


Figure 4.18: Simulation results: distribution of temperature and axial stresses

For a better understanding of the timely development of the stress distribution in the cross section the stress field was analyzed in each time step. In detail, eigenstresses were removed from the stress field and the remaining stresses at the top ($\sigma_N + \sigma_{M,o}$), center (σ_N) and bottom ($\sigma_N + \sigma_{M,u}$) of the wall were drawn against time. The result is shown in figure 4.19.

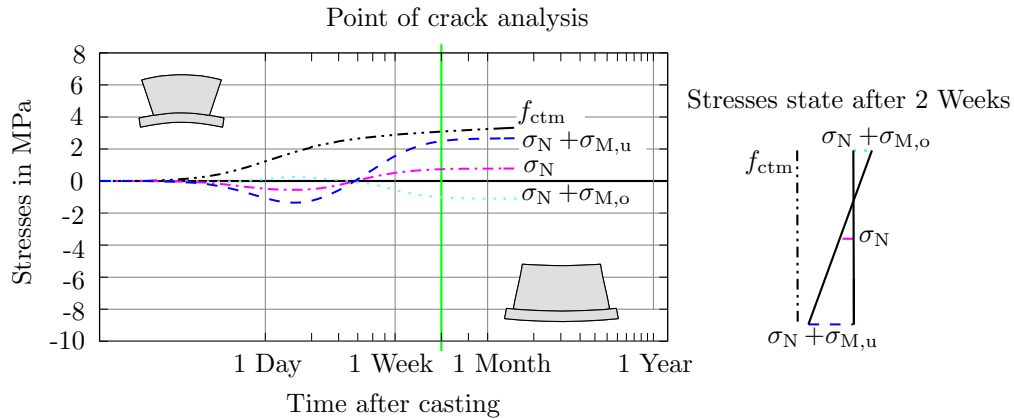


Figure 4.19: Time dependent development of viscoelastic stresses without eigenstresses

It can be seen in figure 4.19 that the prior conclusion that tensile stresses at 30 hours after casting can be seen as a surface problem whereas tensile stresses at temperature equalization belong to a stress resultant in the cross section. The comparison of these stresses with the evolution of average tensile strength f_{ctm} shows further that risk of macrocracking in the present case could only exist at temperature equalization. Thus, the stress state at the temperature equalization represents a much bigger threat for cracking so that all further discussions about cracking are based on this stress state.

4.3.4 Discrete Crack analysis with softening approach

The starting stress state for the crack simulation was taken at the time of temperature equalization (336 hours). However, it is apparent that no cracking will occur in this member since the tensile stresses never exceed the average tensile strength f_{ctm} of the concrete, as shown in figure 4.19.

Figure 4.20 illustrates the final state of the member at temperature equalization. There is a noticeable uplift from self-weight activation but this combined stress state does not cause any cracking in the 3D model.

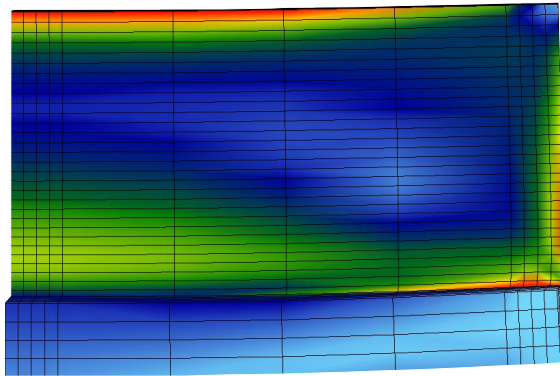


Figure 4.20: Deformation figure of restrained wall at temperature equalization with maximum self-weight activation; still uncracked

Theoretical case with increased hydration heat to provoke severe macrocracking

In order to verify that the developed approach for discrete macrocracking can lead to consistent resulting crack patterns in externally restrained members, this thesis introduces a theoretical case with higher acting forces. This increase of acting forces was induced by a theoretical increase of hydration heat until severe macrocracking is provoked. It is a scientific example which provides theoretical results which are not backed up by observations in construction practice. The resulting stress history without eigenstresses and the comparison with the evolution of average tensile strength f_{ctm} is shown in figure 4.21.

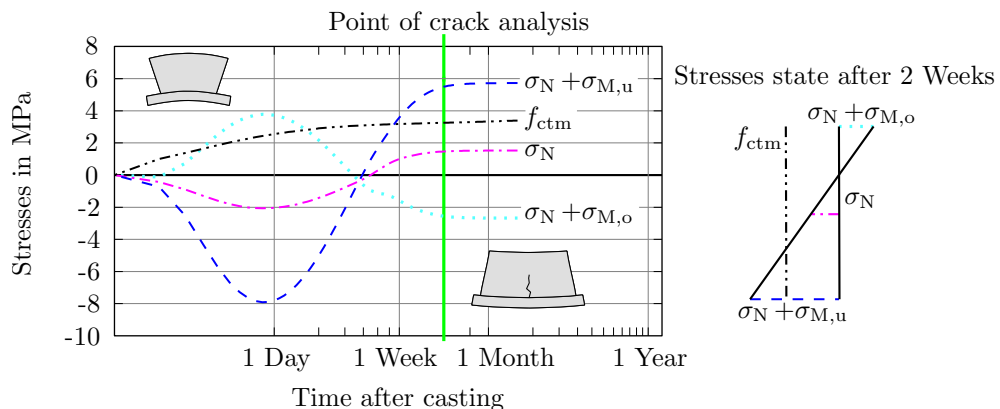


Figure 4.21: Time dependent stress development without eigenstresses

In this case early stresses at the top of the wall exceed the tensile strength at 24 hours after casting already. At the same time, significant parts of the cross section are compressed ($\sigma_N < 0$) so that only locally restricted cracking is to be expected at the top of the wall.

Later, the top of the wall gets compressed over time and therefore these small cracks will even close.

The tensile stresses after temperature equalization exceed also the tensile strength but at the wall bottom. This time the tensile stresses affect significant parts of the cross section ($\sigma_N > 0$) so that distinct macrocracking can be expected. Besides, the determined tensile stresses remain in the same magnitude and a subsequent closing of these cracks cannot be expected.

Altogether, the crack simulation was carried out for the time of temperature equalization. It should be noted at this point that the 3D FE simulation is based on the holistic stress field (including eigenstresses). Figure 4.22 shows the result with respect to (a) the uncracked state on the brink of crack formation and (b) in the equilibrium found after cracking. The macrocrack propagates to 80% of the height of the wall, whereby the cross section is separated over the whole width of the wall in this area.

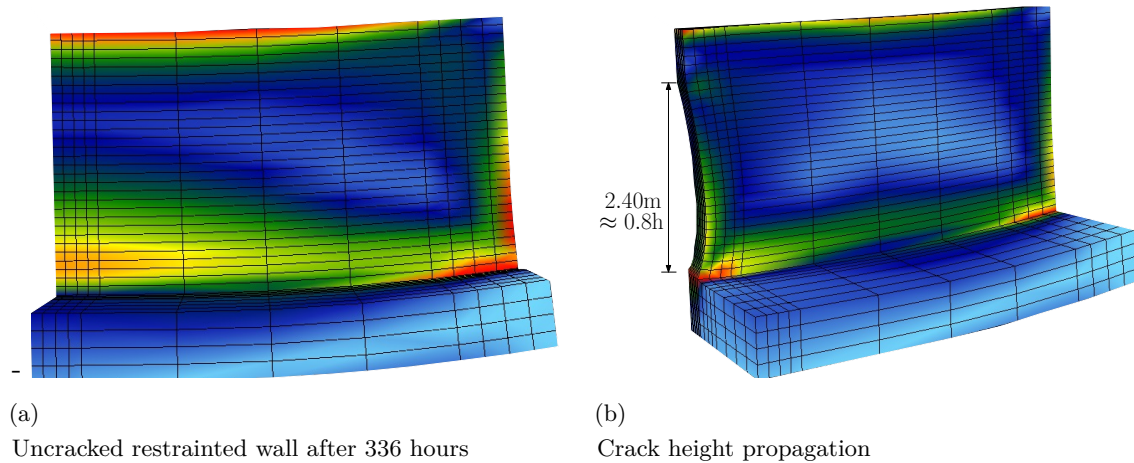


Figure 4.22: Geometric model of restrained wall under temperature load and dead load activation

The resulting crack width was derived from nodal displacements in the longitudinal symmetry section whereby this nodal displacement shows half of the crack width. Figure 4.23 gives the result for the present case. The maximal positive nodal displacements occur on one third of the height of the wall. Besides, it can be seen that the crack width slightly increases in the interior of the wall. Altogether, the maximal displacements amount 0.23 mm which refers to a theoretical crack width of 0.46 mm. Next to the theoretic hydration heat in the present case it should also be emphasized that this crack width refers to a solution without any reinforcement .

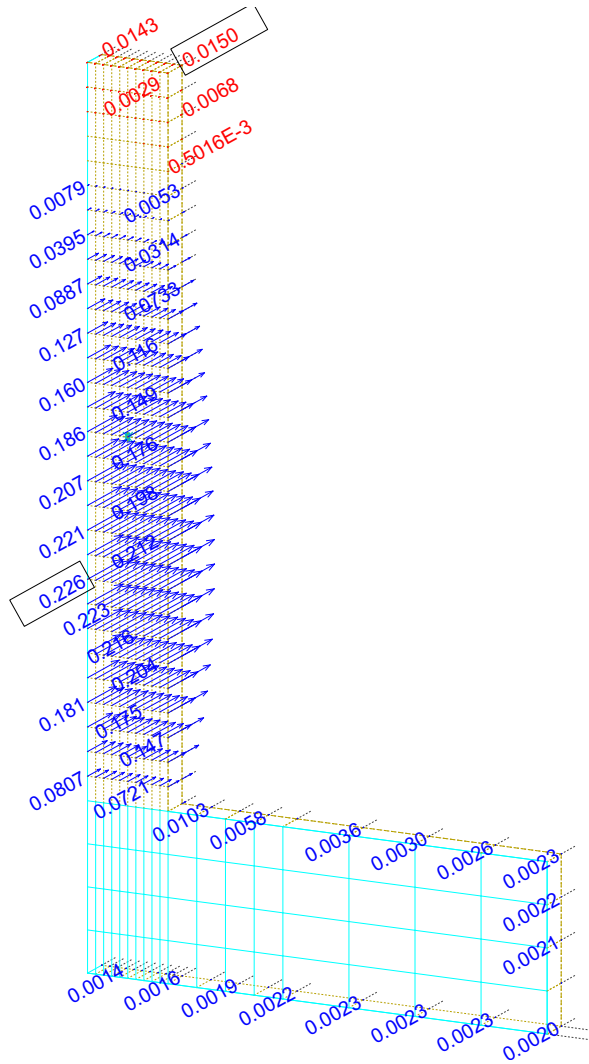


Figure 4.23: Maximal nodal displacements of the considered cross section in mm

5 Discussion

5.1 Crack formation in very thick members with negligible external restraint

The simulation of the block refers to a member with negligible external restraint but significant tension due to eigenstresses. Overall, two modes of failure were determined as illustrated in figure 5.1. The longitudinal crack propagates over the length of the member at its top. This is a result of the great thickness causing a significant interaction between interior and surface region in lateral direction (5.1 a). Besides, transverse cracks can occur propagating over the circumference and reoccurring along the length of the member (5.1 b).

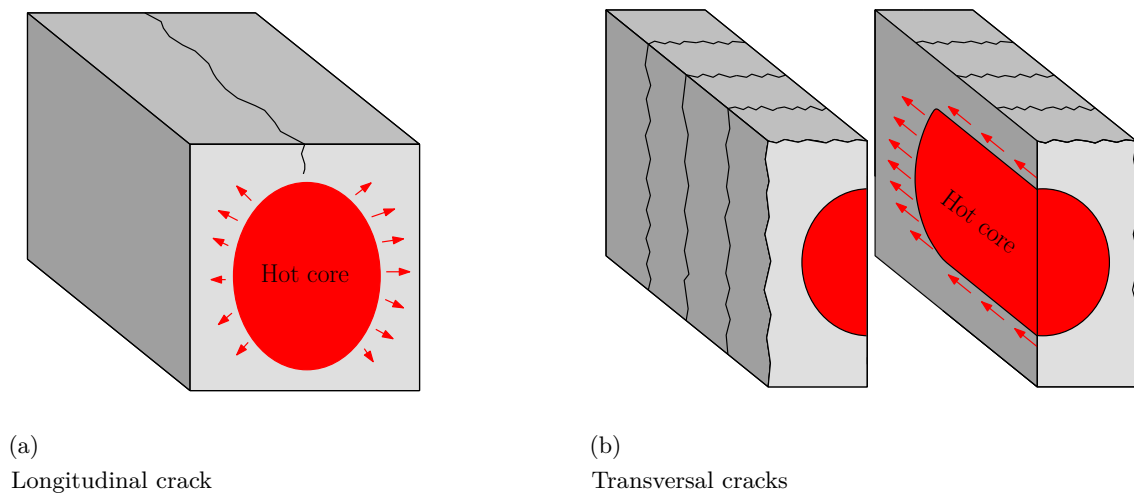


Figure 5.1: Schematic illustration of possible cracking due to thermal expansion of the core

The simulation of associated cracking with the presented approaches provided several results which will be discussed with regard to the following aspects:

- significance of surface cracks depending on the softening
- interplay between two failure planes

The occurrence of surface cracks in the model depends significantly on the consideration of softening. The "element cut off"- approach showed severe macrocracking with remarkable

crack depths in the surface zones. The equilibrium in the stress redistribution was not found before the areas with tension in the uncracked state were cracked. On the contrary, the approach with softening enabled a smooth relieve of stress peaks in the surface area with a gentle stress redistribution. Altogether, only very small cracks with a very small depth were determined.

Concluding, the application of "element cut off" approaches may give conservative results for cracking due to eigenstresses, however, the softening has a significant influence during the stress redistribution. Common eigenstresses in the magnitude of the average tensile strength can hereby fully be relieved without severe crack openings.

Another result of these simulations was the investigation of driving forces of the longitudinal crack on top of the block. In the present case, this investigation was carried out on the simulation with element cut off since this approach enabled a more direct correlation between acting stresses and crack opening. With respect to the determined stress distributions in longitudinal and transverse direction the failure of the springs is to be expected in both symmetry planes, see figure 4.6.

However, the determined crack pattern depends also on the interplay of the 2 failure planes. As shown in figure 5.2 for the case that the failure is initiated in longitudinal direction but no cracking in transverse direction, the transverse stresses are increased. And by this the crack formation in transverse direction is increased, too. However, this effect depends not on the question which crack occurs firstly. Comparative studies with the opposite process (first transverse direction is cracked and longitudinal direction cracks afterwards) give same results.

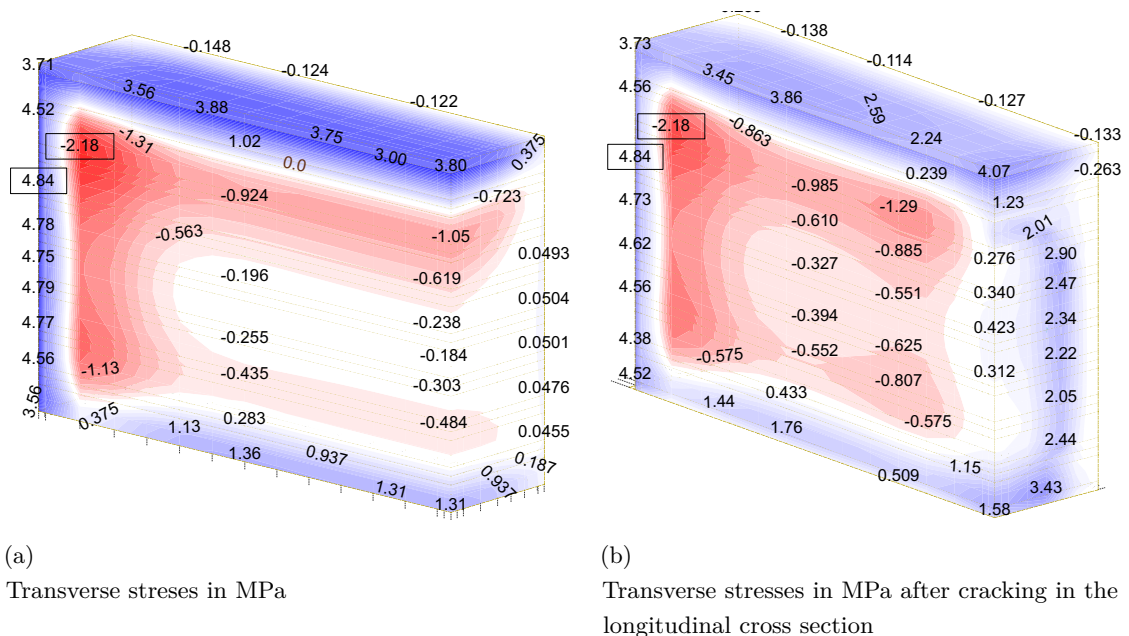


Figure 5.2: Simulation results: distribution transverse stresses at time of max. temperature ($t=90h$)

5.2 Crack formation in walls on foundations

5.2.1 General remarks

As shown in chapter 4, eigenstresses also have a significant role in macrocrack formation of walls on foundations. In case of external restraint, eigenstresses and stresses due to restraint forces are superimposed, however, eigenstresses can be relieved by microcracking and locally restricted cracking in the cross section. Microcracks are generally not visible and their occurrence in the member is only perceived by a local stiffness reduction in the member. Based on the theoretical considerations in [4] this affects the structural behavior in two ways: On the one hand, this stiffness reduction can relieve the member from eigenstresses without the occurrence of distinct macrocracking. On the other hand, this microcracking reduces also the compressive part of the self balanced eigenstresses and thus it can create a much more critical stress state which leads to the real crack formation. Figure 5.3 illustrates this context on basis of the outline in [6].

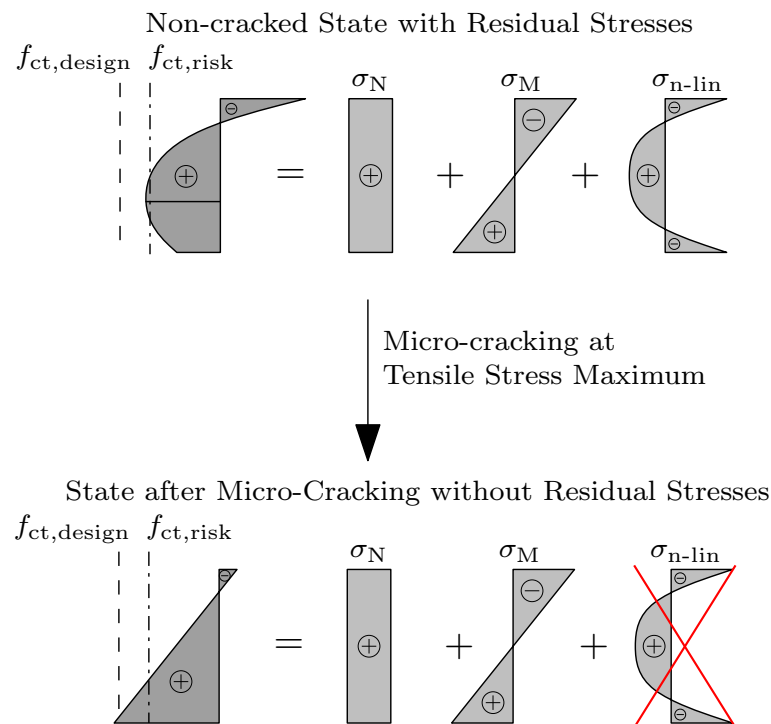


Figure 5.3: Stress distribution and its components before and after microcracking

With regard to the investigated case with theoretical hydration heat, these considerations can be illustrated with figure 5.4. It includes a comparison of the stress state before and after eigenstresses were removed. Altogether, this is a case in which the impact

of non-linear stress components reduce the absolute tensile stresses in the cross section, however, the maximum tensile stresses with eigenstresses are above the tensile strength so that microcracking starts. And without eigenstresses the linear and constant stresses make up for a more critical state.

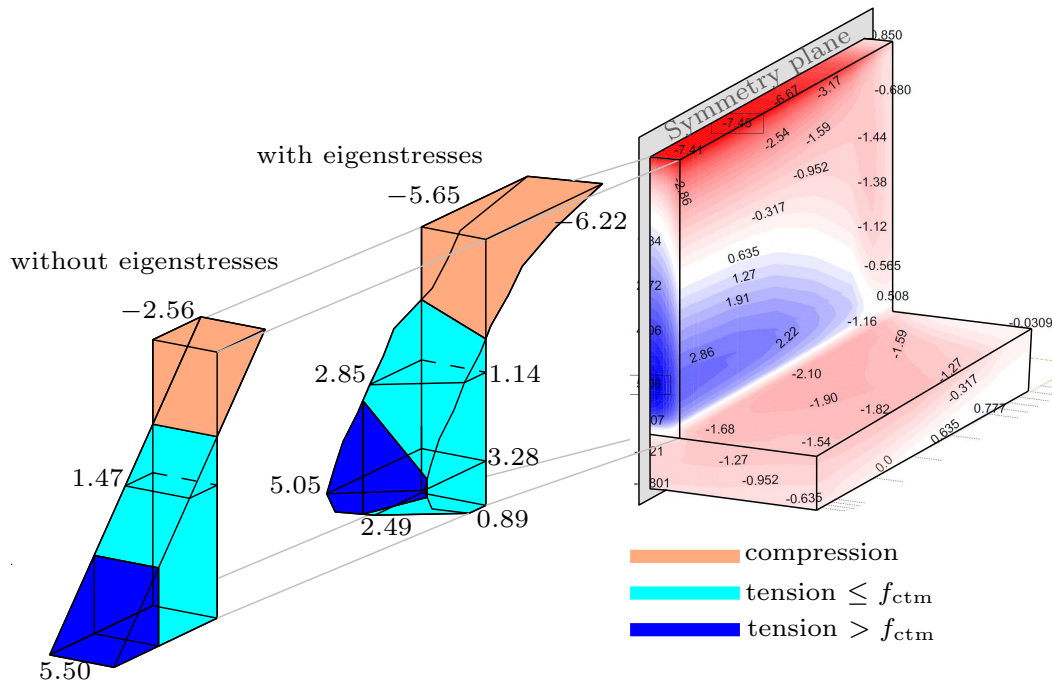


Figure 5.4: Stress distribution in the critical cross section of the wall in MPa

5.2.2 Influence of L/H

Models with the exact same material properties and cross sections but varying lengths present different crack patterns throughout the plane of symmetry. This thesis makes an argument on the influence of length to height ratios, or L/H ratios, on basis of 3 member simulations with the same cross section but different lengths. This section discusses members with L/H ratios of 2.3, 3.5, 7.

Figure 5.5 presents the different crack patterns for these members. This illustration only depicts the walls that are casted on the foundations without the foundation. In qualitative accordance with the postulates made by [1] these results show a increased crack height with increasing L/H ratios. The absolute values are also almost comparable with the results in [1], however, this agreement should not be misinterpreted as verification among each other. The present investigation and the studies in [1] differ significantly in the underlying material behavior. Simulations with the presented approach but with the material behavior

of [1] would indicate significantly less cracking. In accordance with the conclusions in [1] the reason is the difference in underlying softening.

In its current state the presented model simulates only one crack per wall. Conceptual models for the geometrically set reoccurrence of cracks along the wall length can be found in [4]. In combination, this model can act as a tool for prediction of crack height and width along the member length.

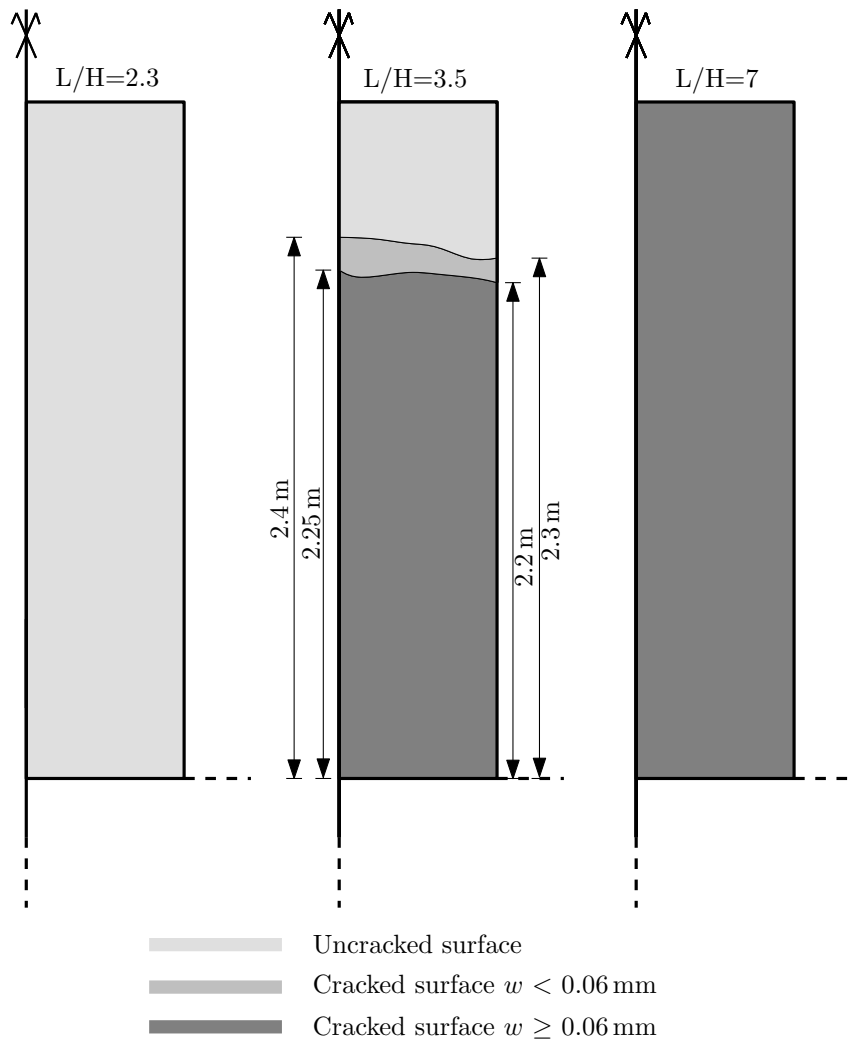


Figure 5.5: Different crack heights based on the L/H ration of the member

5.2.3 Influence of foundation stiffness

According to the considerations in [4] the foundation stiffness affects the restraint stresses in the uncracked wall in two ways: (i) the inner restraint forces depend on the degree of restraint due to cross section compatibility and (ii) the distribution of bending stresses due to self weight activation changes (absolute size of self weight) and zero crossing shifts (centroid of the total cross section shifts).

Figure 5.6 schematically exemplifies these effects on two cases with different foundations with a constantly in the cross section imposed shortening. Their stress state is comprised of a constant and a linear component according to the inner restraint forces as well as additional bending stresses due to self weight activation. Special attention should be given to the latter: in cases where the centroid of the cross section lies above the bottom of the wall, the cross section experiences additional tensile stresses which accelerates crack formation. On the contrary, if the centroid of the cross section lies below the bottom of the wall the additional bending stresses are compressive and thus diminish the initial crack risk of the member. As shown in figure 5.6 these compressive stresses reduce the overall tensile stresses at the bottom of the wall, which is where macrocracks would theoretically start to form. In the event of crack formation, however, this local effect at the bottom of the wall diminishes and cracking proceeds.

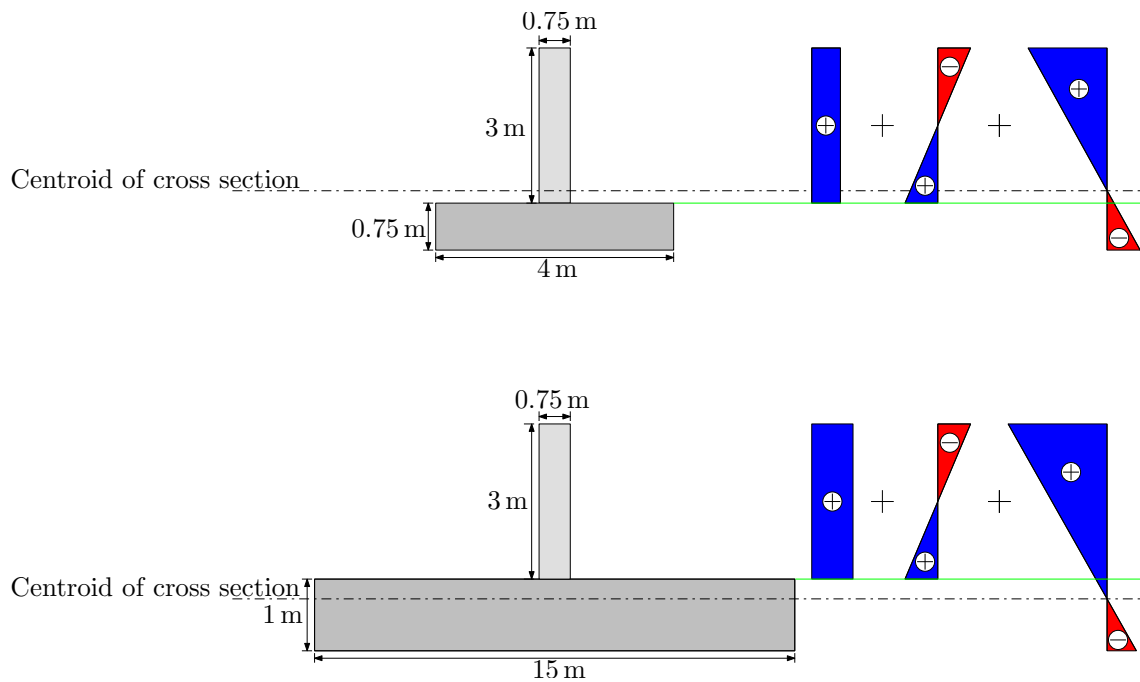


Figure 5.6: Different stress components depending on centroid location

The discrete macrocrack simulation of both cases including a transient temperature field (theoretical case with increased hydration heat) with according stress history confirms these theoretical considerations. The crack height of the wall on a thicker foundation consistently increases, as shown in figure 5.7.

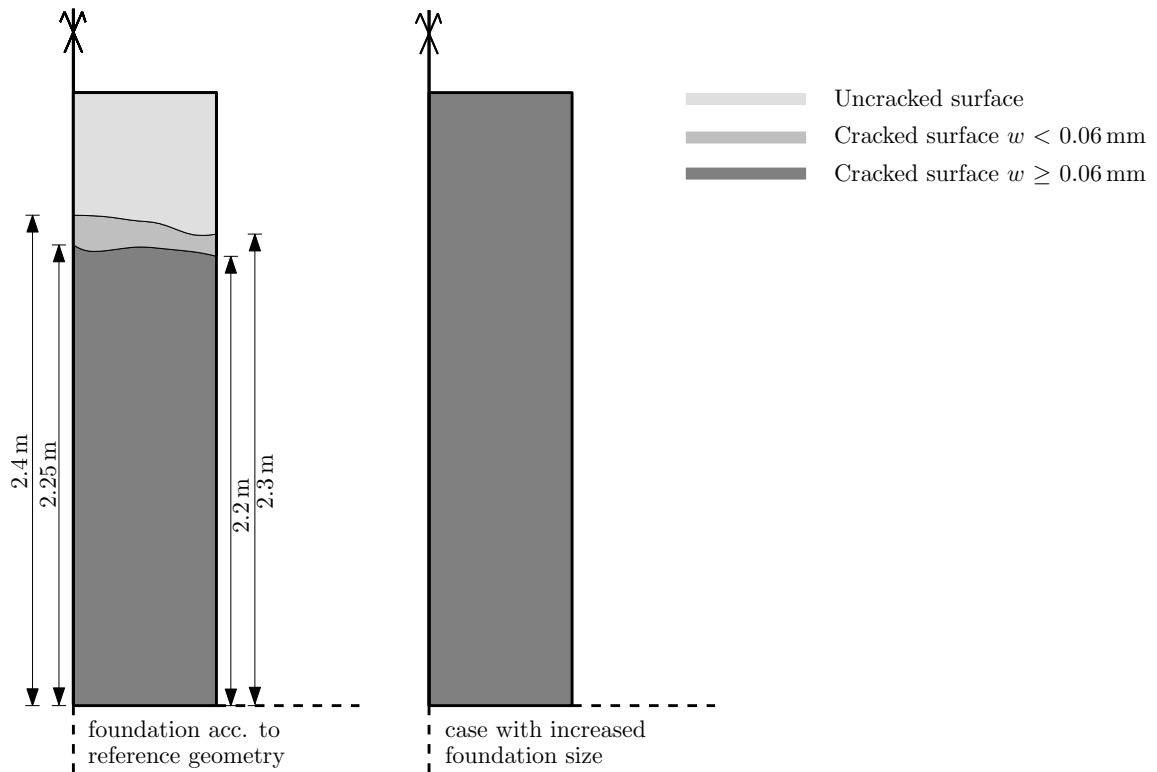


Figure 5.7: Different crack heights based on the thickness of the foundation on which they were casted

In general, larger foundations provide a higher degree of restraint. The presented results in figure 5.7 show increased crack progression with increased foundation thickness and confirm this consideration.

6 Conclusion

This thesis presents the implementation of a discrete plane of failure in thermomechanical 3D calculation models in order to enable the investigation of cracking on the basis of realistic stress states in the decisive cross section of the member. A special emphasis was placed on the consideration of softening behavior in the cracking process of the concrete in order to be able to depict the reduction of the restraint stresses by the initial crack opening. The final model allows systematic investigations of the reduction of eigenstresses due to local failure in the cross section as well as the formation of macrocracks as a result of critical restraint forces. To illustrate this possibility, the second part of this work contains a case study on two typical structural members. On the one hand, a very massive block without significant external restraint was simulated, in which surface cracks can be formed only as a result of the eigenstresses. On the other hand, a thick wall on a foundation was simulated, in which a larger separating cracks occur with increasing length due to the external restraint.

The most interesting result is the influence of adequate softening simulation before physical crack opening. The case study shows that the adequate consideration of softening is of major importance for computational prediction of crack patterns to be expected. Very thick concrete members with small external restraint show usually very high stress peaks in the cross section due to eigenstresses, however, these eigenstresses were significantly reduced due to local softening before physical crack opening. Of course, if the softening is once used up surface cracks with physical opening occur. On the contrary, the simulation of externally restrained members such as a wall on a foundation showed that local stress peaks due to eigenstresses can significantly be reduced by softening - even if significant stresses due to stress resultants are present.

Altogether it can be concluded, that the implementation of a discrete plane of failure in thermomechanical 3D calculation models can be seen as a promising strategy to enable systematic investigations of cracking on the basis of realistic stress states in the decisive cross section of the member.

Bibliography

- [1] A.KNOPPIK-WRÓBEL ; SCHLICKE, D.: Computational prediction of restraint-induced macrocrack patterns in concrete walls. In: *Materials, Systems and Structures in Civil Engineering* Lyngby, Denmark, International RILEM Conference on Materials, Systems and Structures in Civil Engineering Conference segment on Service life of Cement-Based Materials and Structures, 2016, S. S.49–59
- [2] *fib: Modelcode 2010*. 2012. – *fib* Bulletin No. 65, Final draft
- [3] HANSEN, H. F. ; PEDERSEN, E. J.: *Maleinstrument til Kontrol af befors haerding*. Bd. Nr. 1. Nordisk Beton, Stockholm, 1977
- [4] SCHLICKE, D.: *Mindestbewehrung für zwangsbeanspruchten Beton, 2. Aufl.*, Institute of Structural Concrete, TU Graz, Diss., 2016
- [5] SCHLICKE, D. ; TUE, N. V.: Consideration of Viscoelasticity in Time Step FEM-Based Restraint Analyses of Hardening Concrete. In: *Journal of Modern Physics* Bd. 4. SCIRP, 2013, S. S.9–14
- [6] SCHLICKE, D. ; TUE, N. V.: Minimum reinforcement for crack width control in restrained concrete members considering the deformation compatibility. In: *Structural Concrete* Bd. Heft 16. Wilhelm Ernst & Sohn, Berlin, 2015, S. S.221–232
- [7] SCHLICKE, D. ; TUE, N. V. ; KLAUSEN, Anja ; KANSTAD, Tjere ; BJØNTEGAARD, Øyvind: Structural analysis and crack assessment of restrained concrete walls - 3D FEM-simulation and crack assessment. In: *Proceedings of 1st Concrete Innovation Conference* Oslo, Norway, The 1st Concrete Innovation Conference (CIC), 2014, S. 1–10
- [8] SCHLICKE, D. ; TUE, N. V. ; TURNER, K.: Mindestbewehrung und konstruktive Ausbildung von WU-Bauwerken. In: *Betonkolloquium Graz 2016*, A, 3. Grazer Betonkolloquium, 2016, S. S.199–128
- [9] WIESINGER, A. ; JACOBSE, A. ; KOPF, F.: Foundation of the New Botlek Lifting Bridge in the Netherlands. In: *10. Österreichische Geotechniktagung Wien 2015*, A, Österreichischer Ingenieur- und Architekten-Verein, 2015